Achieving Adequate Circulation in Chemical Looping Combustion─Design Proposal for a 200 MW<inf>th</inf> Chemical Looping Combustion

energy&fuels

pubs.acs.org/EF

Article

Achieving Adequate Circulation in Chemical Looping Combustion—Design Proposal for a 200 MW_{th} Chemical Looping Combustion Circulating Fluidized Bed Boiler

Anders Lyngfelt,* David Pallarès, Carl Linderholm, Fredrik Lind, Henrik Thunman, and Bo Leckner

Cite This: *Energy Fuels* 2022, 36, 9588−9615

Read Online

ACCESS | Metrics & More | Article Recommendations

ABSTRACT: Chemical looping combustion (CLC) has unique potential for avoiding the large costs and energy penalties of existing CO_2 capture technologies. Oxygen is transferred to the fuel using an oxygen carrier, thus avoiding contact between air and fuel. Consequently, the combustion products, CO_2 and H_2O, come in a separate stream, and more or less pure CO_2 is obtained after condensation of H_2O. CLC is normally conceived as a dual fluidized bed process, with high gas velocities in an air reactor driving the circulation, similar to circulating fluidized beds (CFBs), except that the material is led to a fuel reactor before being returned to the air reactor. Crucial for the process is the properties of the oxygen carrier and that circulation is sufficient to transfer needed oxygen and heat to the fuel reactor. Comprehensive literature shows successful use of many oxygen carriers in sustained pilot operation. In contrast, the need for reaching adequate circulation in an industrial-scale system has been given little consideration. Normally, a system similar to CFB boilers is assumed to give sufficient circulation. However, literature data indicate that circulation in CFB boilers is 5−50% of what is needed. Measures to provide sufficient circulation may cause difficulties, such as erosion or bed material loss in the cyclone. Here, a circulation system based on collection of the downflow of particles along the walls is proposed, and a design of a 200 MW_{th} combined CLC−CFB boiler based on this principle is presented. Further, operational strategies and the need for flexibility are discussed. The design is focused on making an industrial-scale demonstration boiler, which can be used in CLC operation with different oxygen carriers and different fuels and that can explore different operational strategies to find optimal conditions. It is recommended that the upscaling of the technology aims directly at the industrial scale.

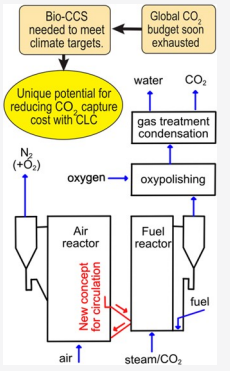

1. INTRODUCTION AND BACKGROUND

The key technologies currently being evaluated and developed for CO_2 capture, e.g., pre-combustion, post-combustion, and oxy-fuel, all suffer from the need for gas separation. These gas separation steps involve significant operational costs as well as large energy penalties, estimated to the order of about 10 percentage points of power plant efficiency, leading to a substantial increase, of around 30% or more, in fuel consumption and plant size. Gas separation technology is generally a mature technology, and no major technology breakthrough is foreseen. This is in great contrast to chemical looping combustion (CLC), where, ideally, no gas separation is needed. CLC is likely the only known technology where a very significant breakthrough could be envisaged for avoiding the large costs and energy penalty of gas separation in CO_2 capture.

In CLC, oxygen is transferred from the air to the fuel using a circulating metal oxide (M_xO/M_x), the oxygen carrier (Figure 1). The high energy requirement and costs of gas−gas separation in CO_2 capture can be avoided because the combustion air and fuel are kept separate and never mixed. Therefore, the exhaust gas stream ideally consists of only CO_2 and H_2O. Thus, CO_2 is readily available after condensation of H_2O.

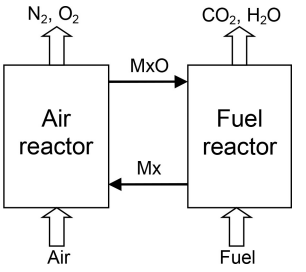

Figure 1. CLC principle.

CLC uses interconnected fluidized bed reactors, where a chemically active bed material, consisting of oxygen carrier

Special Issue: 2022 Pioneers in Energy Research: Anders Lyngfelt

Received: October 22, 2021
Revised: December 16, 2021
Published: February 1, 2022

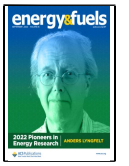

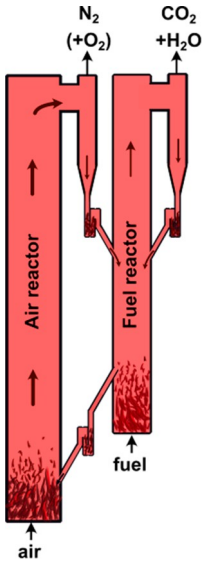

Figure 2. Typical CLC reactor system design with interconnected fluidized beds.

particles, is circulated between two fluidized bed reactors. Figure 2 shows a typical reactor system. A CLC system normally operates at a temperature of 800−1050 °C. CLC was first patented in 1954/1951 in processes to produce CO_2 or syngas[1,2] but forgotten and reintroduced in 1994 as a way to reduce CO_2 emissions.[3] A summary of the state of the art of CO_2 capture is given below.

2. CO_2 CAPTURE, STATE OF THE ART

2.1. Post-combustion Capture. According to the Global CCS Institute, approximately 40 Mt of CO_2 is captured and stored yearly, i.e., around 0.1% of the global emissions. The majority of CO_2 captured comes from industrial processes, where CO_2 is available in concentrated form or where there is a need for removal of CO_2 from gas streams. However, a majority of the global emissions comes from dilute flue gases, and thus far, there are only two major sites where CO_2 can be captured from flue gases: the Boundary Dam in Canada started in 2014 and the Petra Nova in Texas started in January 2017, with a capacity of 1.6 Mt of CO_2/year. Reported costs for these are 110 and 65 US$/t of CO_2.[4] For the Boundary Dam, the reported costs of capital and electricity losses are 87 and 12 US $/t of CO_2, together as 100 US$/t of CO_2.[5] This assumed a 5.5% yearly depreciation, and the sum excludes OM&A, that is, operation, maintenance, and administration, which was not reported.

With the investment as a dominating cost of the capture, it is clear that the discount rate and actual annual capture have important impacts on the costs, cf. Table 1.

Operational costs involve a significant loss in efficiency. The Boundary Dam 3 unit was commissioned in 1970 and produced 139 MW, which was reduced to 110 MW after installation of a new turbine and implementation of CO_2 capture. However, the retrofit also involved increasing the steam temperature and a better turbine, raising the output without CO_2 capture by 11.1 MW to 150 MW.[6] Thus, the capture involves a loss in electricity produced of 27%. No data have been found for the fuel power or energy efficiency, but on the basis of the CO_2 emissions, which are 3600 t/day, and the assumption of a normal lignite, giving approximately 9.8 MJ/kg of CO_2, it is likely that the fuel power is around 405 MW, corresponding to efficiencies of around 27 and 37% with and without CO_2 capture. Thus, the penalty of CO_2 capture would be 10 percentage points. A comprehensive overview of calculated penalties of monoethanolamine (MEA) CO_2 capture indicates a penalty of around 10 percentage points, of which compression accounts for 25−35%.[7] At Petra Nova, a gas turbine is used to operate the carbon capture, which emitted 1.1 Mt of CO_2, or more than a fourth of the 4 Mt captured in total until CO_2 capture was mothballed May 1, 2020 because of falling oil prices.[8] This was because the incomes from enhanced oil recovery (EOR) were not sufficient to cover the operating costs of the unit, which, according to the data above, are not a major part of the costs.

Table 1. Investment Cost, Yearly Captured CO_2, and Specific Cost of Investment

	Petra Nova	Boundary Dam 3	
initial investment	na	1 500 000 000	Can$
initial investment	1 000 000 000	1 153 846 154	US$
nominal CO_2 capture	1 600 000	1 000 000	t/year
capture, best year	1 387 243	792 500	t/year
capture, average	1 180 000	629 395	t/year
net capture,[a] best year	1 005 751	na	
net capture,[a] average	855 500	na	
capital cost, 10% yearly depreciation (average year)	117	183	US$/t
capital cost, 5.5% yearly depreciation (best year)	55	80	US$/t

[a]Emissions from a gas-fired capture plant were subtracted.

The first year of operation of the Boundary Dam, CO_2 capture experienced significant difficulties, but extended operation at the target of 90% capture has been well-demonstrated.[9] At present, the Boundary Dam has reduced its goal of capture from 90 to 65% and reached 64% capture in the last 12 month period.[10] The total amount captured during more than 6 and $^1/_2$ years of operation is 4.1 Mt or 0.62 Mt/year compared to a planned 1 Mt/year or slightly more than half of CO_2 generated.[11] Petra Nova was expected to capture 1.6 Mt/year but seems to be a bit below the target.[8] However, they report having captured 92.4% of the CO_2 stream processed and having high availability through all 3 years, reaching 92−93% in the last year.[12] The remaining difference between projected and planned capture is likely explained by outages not related to the CO_2 capture. Thus, it can be concluded that, even though the Boundary Dam and Petra Nova were the first of their kind, i.e., since the 1980s, there is little doubt that the technology works.

Despite many years of research looking for alternative capture technology, post-combustion capture using MEA or similar alkanolamines has been the dominating solution for capturing CO_2 in flue gases from combustion. The original patent is from 1930, and alkanolamines are still the technology of choice for CO_2 purification.[13] Several plants were built in West Texas to recover CO_2 from boiler flue gas for EOR purposes between 1982 and 1986, using MEA.[13]

2.2. Pre-combustion CO_2 Capture. Pre-combustion involves first the conversion of the fuel to a gas, mainly containing hydrogen and CO_2, and second the removal of CO_2 from this gas stream to produce a carbon-free fuel, i.e., hydrogen. Such hydrogen, if the original fuel is fossil, is called blue hydrogen, in contrast to green hydrogen, which originates

https://doi.org/10.1021/acs.energyfuels.1c03615
Energy Fuels 2022, 36, 9588−9615

Table 2. Estimated Lifetimes of Oxygen Carriers in Pilot Operation[a]

oxygen carrier	pilot	operation (h)	lifetime (h)
	Natural Minerals or Waste Materials		
iron ore[34]	100 kW SF	26	300
iron ore[35]	0.5 kW gas	50	2 000
ilmenite (N)[36]	10 kW SF	11	3 000−9 500
ilmenite (N)[37]	100 kW SF	12	700−800
five Mn ores[38]	0.3 kW gas	17, 7, 27, 29, and 32	80, 110, 330, 1 000, and 2 000
Mn ore (Br)[39]	10 kW SF	10	62
Mn ore (SF-s)[40]	10 kW SF	15	284
two Mn ores[40]	10 kW SF	11 and 16	99 and 109
Mn ore (calc)[41]	10 and 100 kW SF	23 and 33	200−745
Mn ore (SF-a)[42]	100 kW SF	52	100−400
LD slag[43]	0.3 kW gas	20	170
LD slag[43]	10 kW SF	28	110−170
	Manufactured Materials, $CaMnO_3$ Based		
$CaMn_{0.9}Mg_{0.1}O_{3-\delta}$[44]	10 kW gas	55	12 000
$CaMn_{0.775}Mg_{0.1}Ti_{0.125}O_{3-\delta}$[45]	0.5 kW gas	60	500−2 000
$CaMn_{0.775}Mg_{0.1}Ti_{0.125}O_{3-\delta}$[46]	10 kW gas	99	9 000
C28-E1S2[45]	0.5 kW gas	60	500−2 000
C28-E1S2[47]	10 kW gas	24	5 000
C28-901[47]	10 kW gas	110	700
C28#902-1,2[48]	1 MW gas	50	500
	Other Manufactured Materials		
$CuO/MgAl_2O_4$[49]	0.5 kW gas	50	5 000
CuO/ZrO_2[50]	0.5 kW gas	30	1 500
$Mn_3O_4/SiO_2/TiO_2$, 6:2:1[51]	10 kW SF	32	5 600
$NiO/NiAl_2O_4/MgAl_2O_4$[52]	10 kW gas	1 016	33 000

[a]Operation is time of operation with fuel. SF denotes solid fuel and SF- denotes sintered fines.

from renewable sources, or black, brown, or gray hydrogen, which comes from various fossil fuels where CO_2 has not been captured.

In the case of solid fuel, pre-combustion requires a gasification step, where the fuel is partially oxidized by oxygen, followed by additional steps to convert the gas to CO_2 and hydrogen before the separation of these. Thus, two steps of gas separation are needed: oxygen production and H_2/CO_2 separation. The process has the attractive feature of generating a gaseous fuel, which opens up for high energy efficiency because a combined gas turbine and steam turbine cycle can be used. Gasification of solid fuels is, however, more costly and difficult than normal combustion. Therefore, only a few integrated gasification combined cycle (IGCC) plants have been built. The 582 MW_e Kemper project is both the largest IGCC ever built and the largest CO_2 capture project from power production ever. It was planned to capture 65% of CO_2 or 3 Mt annually. The cost of the plant increased from an estimated 2.4 to 7.5 B$, making Kemper the most expensive power plant ever built.[14] After a successful production of 95 500 tons of CO_2 and 165 000 MWh, corresponding to 1 and $^1/_2$ weeks of full-load operation, the plant stopped using coal gasification.[15] Despite the gigantic investment, the power plant switched to operation with natural gas without CO_2 capture.

Steam methane reforming (SMR) is the most common source of hydrogen. The process involves the endothermic reaction of steam and methane, i.e., natural gas, to produce a gas consisting of H_2, CO_2, H_2O, CO, and some unreacted CH_4. This gas is led to a water−gas shift (WGS) reactor, where H_2O and CO react to form more CO_2 and H_2. Finally, H_2 is separated from the gas, and the remaining off-gas is burnt to provide the energy needed for the endothermic reaction in the catalyst-filled steam methane reformer tubes. To produce blue hydrogen, diluted CO_2 from the combustion chamber needs to be captured. Part of CO_2 can also be captured from the more concentrated off-gas. Natural gas processing is the major source of the 40 Mt of CO_2 being captured and stored worldwide.

2.3. Oxy-fuel Combustion. The idea of oxy-fuel is to burn a fuel in a mixture of oxygen and recycled flue gas, thus avoiding nitrogen in the combustion air. Ideally, the combustion products will be CO_2 and water vapor, and the latter can be removed by condensation. The energy penalty and costs come from the production of oxygen for the process. Fundamentally, the theoretical gas separation work is close to that of post-combustion because it involves similar amounts of gas and reasonably similar concentrations. It is not clear why this separation process would be preferred, because the properties of the nitrogen and oxygen molecules are more similar than those of carbon dioxide and N_2/O_2. On the other hand, oxygen production from air is a well-established technology, albeit not in the scale of power production. An important difference is that the energy needed for gas separation is electricity and not heat. For a power plant, the total energy penalty is expected to be similar to that of post-combustion.[16]

In contrast to post-combustion capture and pre-combustion capture, oxy-fuel combustion has never been tested on a large scale. However, demo plants have been built, e.g., Schwarze Pumpe 30 MW_{th}, Ciuden 30 MW_{th}, NET Power 50 MW_{th}, and Callide 30 MW_e, with the latter having 10 000 h of operation.[17]

If green hydrogen production using electrolyzers, is used at scale, the electrolyzers will produce large amounts of oxygen as

https://doi.org/10.1021/acs.energyfuels.1c03615
Energy Fuels 2022, 36, 9588−9615

a byproduct. This could be an opportunity for oxy-fuel CO_2 capture. The experiences from oxy-fuel are important for CLC, because oxygen may be needed to reach full conversion of the gas leaving the fuel reactor (FR).

2.4. Chemical Looping Combustion. In 2003, when the process was still no more than a paper concept, a rapid development started with the first demonstration of this new combustion technology during more than 100 h of successful operation in a 10 kW prototype operating with natural gas reaching 99% gas conversion and 100% CO_2 capture.[18,19]

Recent comprehensive overviews of work on oxygen carrier materials are not available, but earlier reviews[20−22] included 200 publications on experimental work covering approximately 900 materials, mostly in the laboratory. Recent overviews of operation in chemical looping combustors in total include 49 units in sizes from 300 W to 3 MW presented in 222 publications.[23−29] The work comprises many oxygen carrier materials and close to 12 000 h of operational experience, with Chalmers University being a main contributor, with more than 4000 h of operation using more than 70 materials.

Oxygen carrier materials used include manufactured monometallic oxide systems, e.g., oxides of Ni, Fe, Mn, Cu, and Co, as well as a number of combined oxide systems, primarily combined Mn oxides. Further, more than 3400 h of operation has been reported for low-cost natural ores, i.e., ilmenite ($FeTiO_3$), manganese, and iron ore.[27] Thermodynamics and oxygen carrier capacity are well-established for these systems.[30,31] Reviews of material integrity are rare[32] but indicate a clear correlation between attrition test results and actual attrition in CLC operation, whereas crushing strength tests were less correlated. Many works have estimated the oxygen carrier lifetime from the loss of fines (see Table 2). For low-cost materials, a lifetime of a few hundred hours would be sufficient to reach reasonable costs of the bed material.[33] Manufactured materials produced from pure chemicals would be an order of magnitude more expensive and need a correspondingly longer lifetime. Thus, natural minerals may cost a few hundred €/tonne, whereas comparable commercial particle materials, like fluid catalytic cracking (FCC) catalysts, are at a few thousand €/tonne. Potentially, manufactured calcium manganate-type materials could be less costly if produced from low-cost limestone and manganese ore.

In addition to lifetime, the effect of long-term operation and interaction with fuel ash is important. Long-term operation with oxygen-carrier-aided combustion (OCAC) has been performed in industrial-scale boilers, including 20 000 h burning municipal solid waste in a 75 MW circulating fluidized bed (CFB) boiler[53−55] and 500 h with a mix of recycled waste wood and wood chips in a 125 MW CFB boiler.[56] In addition, there is 830 h of OCAC operation with ilmenite and wood chips in a 12 MW CFB.[57] Investigation of the oxygen carrier showed that the reactivity increased with time of operation to reach a maximum between 60 and 150 h but had somewhat lower reactivity after 320 h.[58] In the same boiler, a manganese ore has been used in operation during 580 h, with an estimated oxygen carrier lifetime of more than 1000 h.[59]

The pilots used are adequate for the evaluation of oxygen carrier materials. They show a large variety in layout,[28,60,61] although the pilot designs cannot be directly translated to the industrial scale.

Operation with solid fuels in CLC has been performed in 20 units and involves more than 3700 h, starting in 2006 with a solid-fuel 10 kW chemical looping combustor.[26,27,36,60,62] When solid fuels are used, the oxygen carrier can react with the volatiles but not directly with the char. Instead, the oxygen carrier reacts with syngas produced from the gasification of char. The conditions for gasification in the FR are good, with high steam and CO_2 concentrations and low concentration of combustibles, such as H_2, known to inhibit gasification. Normally, high temperatures are used, e.g., 970 °C. Experiences from pilot operation indicate, somewhat counterintuitively, that char may be less of a problem in CLC than the volatiles. Thus, pilot operation with coal shows that low loss of char from the FR to air reactor (AR) and filter is possible, whereas gas conversion is incomplete using low-cost oxygen carriers.[24]

At the same time, pilot operation shows almost complete gas conversion when only char is left in the system, e.g., after a fuel stop, but much lower conversion with high-volatile fuel (Figure 3). The high conversion of syngas from char can be explained

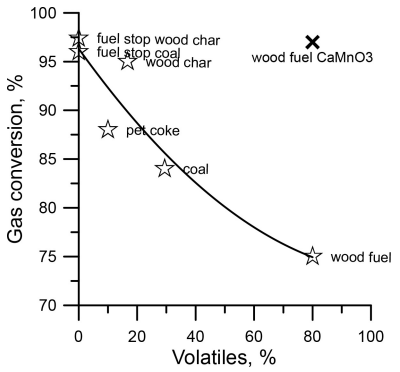

Figure 3. Gas conversion versus volatiles in fuel.

by the char being well-mixed with the dense particle phase, whereas the low conversion of volatiles is associated with gas bypassing the bottom dense phase. However, much higher conversion is expected in a full-scale unit, where the riser can be 10 times higher, providing better gas−solids contact in the riser. It should be noted that incomplete gas conversion is remedied by oxy-polishing, i.e., oxygen addition downstream of the FR, albeit at a cost. Although there are oxygen carrier materials able to reach full gas conversion, these are normally more expensive, and incomplete conversion with a less costly material could be optimal, at least with ash-rich fuels.

The fuel size is important; with centimeter large particles, much char is lost to the AR, whereas pulverized coal gives substantial loss of char with the outgoing gas stream. Intermediate size coal of 0.1−0.3 mm, however, gives low losses.[24] Thus, coal size is much smaller than in normal CFB operation, which could be expected to lead to a significantly reduced size of the ash particles formed. The separation of ash and oxygen carrier would also be greatly facilitated if the majority of the ash leaves the system as fly ash. In addition, it is possible to use magnetic separation of ash and oxygen carrier.[58]

At present, experience of operation with biomass is limited, although some successful operation has been published.[41,63,64] Gas conversion decreases with the content of volatiles and is therefore much lower with biofuels.[24] Figure 3 shows the best results from the 100 kW CLC at Chalmers University with the ilmenite ore (stars) and best result with calcium manganite (cross).[64] It is clear that calcium manganite ($CaMnO_3$) can reduce unconverted combustibles dramatically. Results with

https://doi.org/10.1021/acs.energyfuels.1c03615
Energy Fuels 2022, 36, 9588−9615

biomass are further discussed in section 9, Fuel Reactor Design.

2.5. NO_x Formation in CLC. An additional advantage with CLC is that the effluent from the AR, which is essentially what will come out of the chimney, should be free from contaminants as long as no char leaks from the FR with the solids circulation. The absence of flame combustion with locally high temperatures in any of the reactors means that thermal NO_x cannot form. With the fuel being absent in the AR and with no nitrogen in the FR except for small amounts from fuel N, prompt NO_x should not be possible. Finally, the normal path for NO_x formation from fuel N is closed for lack of gaseous oxygen in the FR. Instead, the only mechanism for NO_x formation is from fuel nitrogen reacting with the oxygen carrier or from fuel NO_x being formed in the oxy-polishing step. In the FR, the thermodynamic equilibrium concentration of NO is less than a thousandth of a part per million (ppm) because of low nitrogen and the absence of free oxygen. However, reduced nitrogen species in the volatiles released in the FR react with the oxygen carrier to form NO.[65] Thus, measurements with coal in CLC found concentrations in the range of 200−2000 ppm.[37,66] These concentrations are higher than what is typical of normal CFB boilers. For a comparison of total amounts, these concentrations should be multiplied by a factor of around 3.5 because they are concentrated in the smaller flow from the FR. It was clear that NO is very sensitive to reaction conditions, and high concentrations were generally associated with high conversion of the combustible gases. It is also clear that the gas from the FR contains ammonia.[37] Data for biomass are difficult to find, although Pérez-Astray et al. report around 100−150 ppm for pine sawdust, almond shells, and olive stones.[67]

There are no dedicated studies of the fate of nitrogen species in the post-oxidation chamber, but literature data suggest that NO could be significantly reduced,[37] e.g., by reaction of NO and NH_3 to N_2. However, the absence or very low concentration of nitrogen in combination with very low oxygen concentration in the post-oxidation chamber gives a low equilibrium concentration. Thus, with the assumption of 0.5% O_2 and 0.5% N_2, corresponding to fuel nitrogen, the equilibrium NO concentration is 16−60 ppm at temperatures in the range of 1200−1500 °C. Consequently, thermal NO_x formation is not expected to give higher NO concentrations, and higher temperatures in the post-oxidation chamber would rather be expected to facilitate an approach to equilibrium.

Thus, NO_x formed will be concentrated in the smaller stream of mainly CO_2 from the post-oxidation chamber, where it is estimated that it can be addressed at a third of the cost of presently available flue gas NO_x reduction technologies, like selective catalytic reduction (SCR) and selective non-catalytic reduction (SNCR).[68]

2.6. CLC Costs. The costs of CO_2 capture with CLC of solid fuels was as low as 10 €/t according to a first estimate made by boiler maker Alstom in the European Union (EU) project ENCAP.[69] Later studies also show low costs: 16−26 €/tonne,[33] 26 €/tonne,[70] and 20−30 €/tonne[71] for coal and 24 €/tonne for biomass.[72] Thus, CLC has the potential to lower the cost of CO_2 capture by 50−80% compared to conventional CO_2 capture.

CO_2 compression, the highest cost in Table 3, is inevitable for any CO_2 capture technology. The other important cost is oxy-polishing, i.e., oxidizing unconverted combustibles with oxygen. This is the key cost to address. Note the low added cost of a CLC boiler, that is, in comparison to a CFB boiler. The main added cost is the FR, cf. Figure 2, and consists of the well-insulated reactor walls with an expected cost of 1500 €/m^2. For a 200 MW_{th} unit with 800 m^2 walls, the added cost would be 1.2 M€, corresponding to a cost of 0.12 M€/year with 10% yearly depreciation. With 0.4 Mton/year of CO_2 captured, the specific cost becomes 0.3 €/ton of CO_2. Thus, the added cost relating to the boiler system could be very low. Consequently, the key focus for cost reduction is gas conversion, although it is important to maintain low oxygen carrier cost.

Table 3. Cost Estimation for CLC[33]

	€/tonne of CO_2
CO_2 compression	10
oxy-polishing	6.5
boiler cost	<1
oxygen carrier	2
steam and hot CO_2 fluidization	0.8
coal grinding	0.2
lower air ratio	−0.5
total	20

2.7. Chemical Looping with Oxygen Uncoupling (CLOU). The lower gas conversion in CLC with biomass can be addressed by CLOU. In CLOU, the oxygen carrier releases gaseous oxygen, which reacts with char and volatiles.[73] This is in contrast to normal CLC, where the oxygen carrier reacts with fuel gases.

CLOU requires an oxygen carrier with the ability to both react with oxygen in the AR and release oxygen in the FR. This is possible for oxide systems having an adequate equilibrium concentration of oxygen, i.e., below around 5%, which represents the minimum in the AR, and high enough to release oxygen in the FR, where the oxygen concentration is kept very low by the reaction with fuel. To be technically relevant, the oxide system should preferably have an equilibrium oxygen concentration of around 1−3% at temperatures of around 900−1000 °C. Known systems that fulfill this criterion are copper oxide and some combined manganese oxides.

Mattisson et al. identified the potential for CLOU with copper oxides (CuO/Cu_2O).[73−75] However, copper oxides have two difficulties: first, the possible reduction to Cu, which has a low melting temperature, and second, the high cost. Combined manganese oxides can also be used in CLOU, although having lower oxygen release capacity compared to copper oxides.[76−78] This group of materials includes combined manganese oxides with iron, nickel, silicon, calcium, and magnesium.[31,79−84] Further, ternary systems have been examined.[85] Best results thus far were obtained with calcium manganite, $CaMnO_3$, a perovskite with oxygen-releasing properties. More than 700 h of operation with calcium manganate in seven different pilots of 0.3−1000 kW, mostly with gaseous fuels, clearly demonstrates that these materials show a long lifetime, high performance, and under good conditions, even full gas conversion.[44,46,86−98] Natural gas has been in focus for calcium manganite research. The sensitivity to sulfur makes the material less suitable for coal but is no problem with biomass, and gas conversion was raised from 75 to 97% with calcium manganate when using biomass fuel in a 100 kW CLC pilot (Figure 3).[64]

https://doi.org/10.1021/acs.energyfuels.1c03615
Energy Fuels 2022, 36, 9588−9615

$CaMnO_3$ does not have to be pure; part of the operation reported has been performed with calcium manganite made from impure raw materials, and various additives, Fe, Mg, Ti, etc., are often used. Manufacture of calcium manganate from low-cost manganese ore and lime was demonstrated in the EU project SUCCESS.[47,99] Although there is an extra cost for producing calcium manganite compared to natural ores often used for solid fuels, this might be motivated, given the improvement in gas conversion, reducing or even eliminating downstream costs for oxygen polishing to remove combustibles from the CO_2 stream.

For gaseous fuels not containing sulfur, the bed material will not be contaminated by fuel ash and sulfur, and the material lost as fines may be used for production of bed material of an adequate size. Consequently, manufactured materials are more likely to be relevant for such fuels.

2.8. Energy Penalty in Gas Separation and Compression. The energy penalty of CO_2 capture includes the penalty of gas separation to produce CO_2 at ambient pressure of sufficient purity for transport and storage and the penalty of CO_2 compression from ambient pressure to the pressure needed for transport and storage, at around 100 bar.

Assuming isothermal conditions, i.e., removal of the heat generated by compression, and ideal gases, the theoretical compression work (J/mol) is given by

$$W_{th} = -RT \ln(p_1/p_2) \quad (1)$$

where R is the gas constant (J mol^{-1} K^{-1}), T is the absolute temperature, and p_1 and p_2 denote initial and final pressures. The theoretical work to compress the gas from 1 to 100 bar is thus 0.255 MJ/kg of CO_2. The isentropic efficiency, η_{is}, is the ratio of the theoretical work and the actual work needed. Thus

$$W_{act} = W_{th}/\eta_{is} \quad (2)$$

Isentropic efficiencies of compressors are in the range of 70−85%. An efficiency of 77.5% yields the needed compression work as 0.33 MJ/kg of CO_2. Assuming ideal gas, however, is not correct at higher pressures where carbon dioxide is liquid or supercritical, depending upon the temperature, and therefore, the theoretical compression energy is overestimated. The non-ideal behavior is more pronounced at lower temperatures, which means that the compression energy is much more sensitive to the cooling temperature than in eq 1. Thus, a more accurate calculation of compression energy for 1 to 100 bar showed an increase from 0.306 to 0.366 MJ/mol of CO_2, as the temperature increased from 20 to 40 °C.[100]

For ideal gases, the theoretical energy needed to separate a mixture of two gases a and b is

$$W_{th,sep} = -RT(x_a \ln(x_a) + x_b \ln(x_b)) \quad (3)$$

where x_i is the molar ratio of gas i. For CO_2 concentrations typical of coal and biomass fuel combustion, e.g., 15.5 and 17%, the work is 0.154 and 0.148 MJ/kg of CO_2, which is less than half of the actual compression work. For direct air capture (DAC), that is, capture of CO_2 from ambient air, the theoretical separation energy is more than 3 times higher, 0.488 MJ/kg of CO_2.

In contrast to compression, gas separation processes are far from ideal. The major energy penalty of the MEA process is the heat needed to regenerate the absorbent, which is 3.9 MJ/kg of CO_2.[101] The Petra Nova plant uses a solvent called KS1, reported to have a regeneration energy of 2.94 MJ/kg.[102] This can be compared to the heating value of solid fuels, which is 10.3 and 10.8 MJ/kg of CO_2 for dry biomass and coal and 8.6 MJ/kg of CO_2 for biomass with 50% moisture. In power plants, low-pressure steam can be used to generate the heat needed for regeneration of the solvent, which translates into a lower penalty with respect to electricity. Typically, the total electricity penalty including compression is around 10% of the fuel heating value, which means that around a fourth of the electricity produced is lost in the post-combustion process.

For oxy-fuel, the electric penalty of gas separation is around 0.9 MJ/kg of O_2 assuming 99.5% purity,[103,104] which translates to 0.65−0.76 MJ/kg of CO_2 for biomass and coal. Together with CO_2 compression, this gives 0.98−1.1 MJ/kg of CO_2. This is 10% of the fuel heating value for coal or biomass with 20% moisture.

For CLC, the energy penalty in addition to compression mainly comes from oxy-polishing and production of steam needed for fluidization of loop seals and the FR. This has been estimated to around 0.1 MJ/kg of CO_2.[33] Figure 4 illustrates the penalties. Note that electric power is compared to low-temperature heat (MEA).

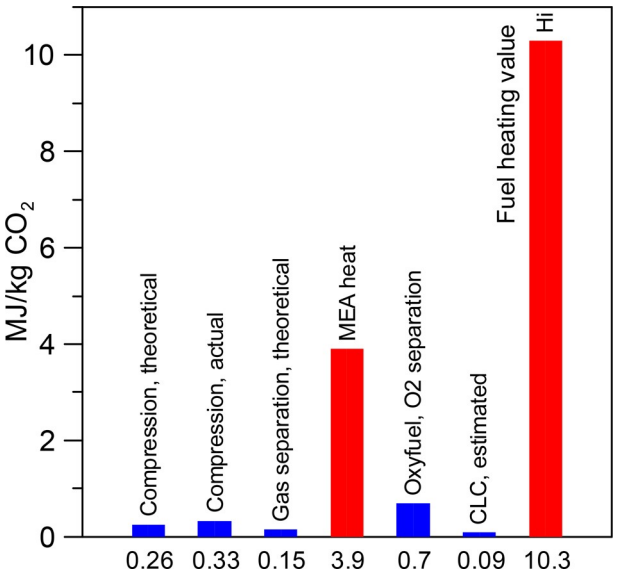

Figure 4. Energy penalties of CO_2 capture. For comparison, H_i, the fuel heating value of dry biomass per kilogram of CO_2, is included. Blue bars indicate power, and red bars indicate heat.

For comparison, the reported energy need for direct air capture, e.g., Climeworks' process, is 7.2 MJ_{heat}/kg of CO_2 plus 2.3 $MJ_{electricity}$/kg of CO_2.[105] Thus, the energy needed to remove a given amount of CO_2 from the atmosphere equals the amount of CO_2 produced by a boiler fired with solid fuels producing this energy, given a flue gas loss of 90%.

3. APPLICATIONS OF CHEMICAL LOOPING COMBUSTION

The most near-at-hand applications of CLC would use solid fuels. This is because the technology has important similarities to conventional combustion of solid fuels in CFB boilers. The key differences between a CLC and CFB boiler are the need for a FR and the use of an oxygen carrier as bed material.

3.1. Coal. With coal, the technology could potentially not only capture CO_2 at low cost but also offer 100% CO_2 capture and possibly eliminate NO_x and SO_x emissions. This is because

https://doi.org/10.1021/acs.energyfuels.1c03615
Energy Fuels 2022, 36, 9588−9615

these streams will come in the concentrated CO_2 stream and, in any way, need to be removed before storage. A techno-economic analysis indicated that integrated NO_x and SO_x removal from a concentrated CO_2 stream could reduce the cost to 640 €/ton compared to 2900 €/ton for wet flue gas desulfurization and selective catalytic NO_x reduction.[68]

3.2. Biomass. With biomass, CLC could provide negative emissions at reduced cost, but CLC may also come with other important advantages. As with coal, low or eliminated NO_x emissions are one advantage. Another potential advantage is associated with the important difficulties imposed by the aggressive alkali ash components in many biomass fuels. If the alkali is mainly released in the FR and avoided in the AR, this could give a significant reduction of maintenance costs as well as higher efficiency, cf. Figure 5.

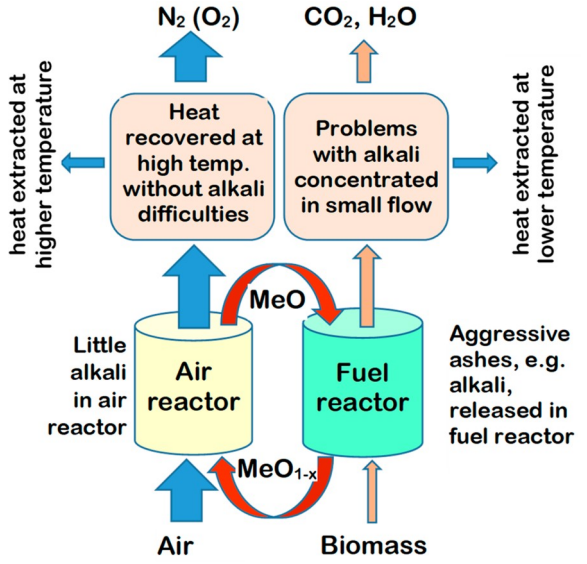

Figure 5. Possible advantages with respect to alkali contaminants.

Furthermore, the oxygen carrier may neutralize potassium by absorbing it. The fate of alkali has been investigated in OCAC in long-term operation in an industrial-scale CFB. Silica sand, which is currently the most common bed material in fluidized bed combustion of biomass, captures potassium on the particle surfaces, forming sticky compounds with the silica. For this reason, the sand needs to be continuously exchanged. Ilmenite, on the other hand, captures potassium throughout the structure in the form of non-sticky titanium silicates and has shown an even distribution of potassium over the particle cross section after 364 h of operation.[106] Similarly, the fraction of potassium in the bed material when using a manganese ore was seen to increase during 172 h of operation.[107]

The advantages with ilmenite in OCAC involve the oxygen-buffering capacity, which may reduce both CO and NO_x, but may also reduce ash-related problems. Thus, in operation of a 12 MW CFB, it was found that soot blowing of the flue gas channel downstream of the cyclone outlet was not needed, as shown in Figure 6. When operated with sand, the temperature of the flue gas leaving the economizer increases because of ash deposits building up, and recurrent soot blowing is needed to return to the desired temperature. During the 19 days of ilmenite operation, no soot blowing was needed.

Further, in measurements at three different CLC pilots, with two different oxygen carriers and different biogenic fuels,

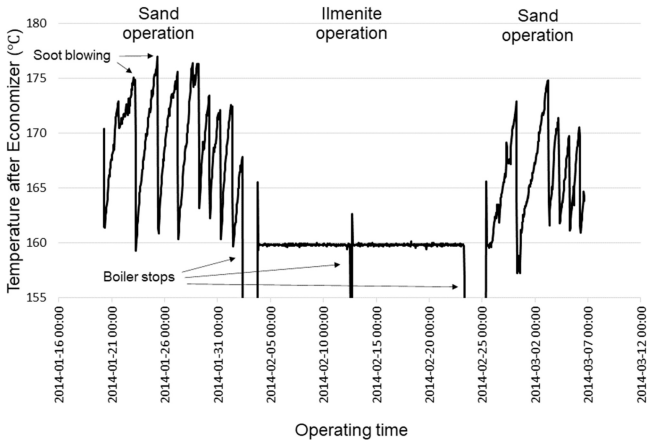

Figure 6. Gas temperature after the economizer of a 12 MW_{th} CFB operated with either sand or ilmenite.

including high alkali fuels, like straw-based and alkali-enriched fuel, only a few percent of the added alkali was found in the effluent streams.[64,108,109] Accumulation of alkali in the bed material supported this observation. Alkali and CLC are further discussed in ref 26.

3.3. Blue Hydrogen by Combining CLC with SMR. CLC can be combined with SMR if CLC is used to supply the heat for the SMR and to burn the off-gas from the SMR (see Figure 7).[110,111] This process holds remarkable advantages

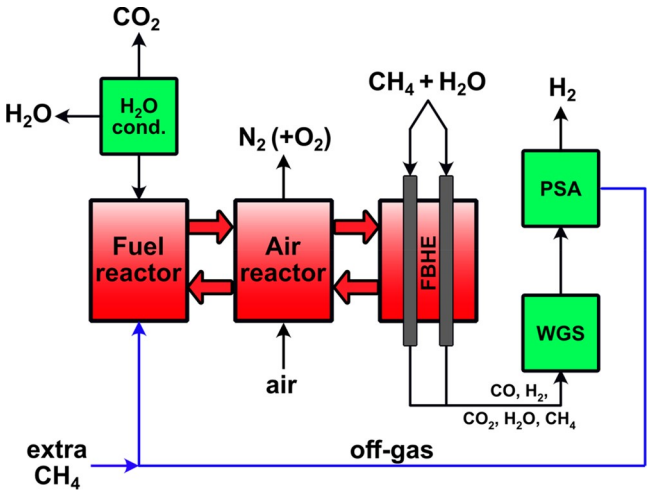

Figure 7. Steam methane reforming and chemical looping combustion (SMR−CLC).

compared to conventional SMR because the exit temperature from the combustion chamber can be reduced from, e.g., 1200 to 935 °C because of the much more effective heat transfer in fluidized bed heat exchangers (FBHEs). Furthermore, local hot spots on the expensive catalyst-filled reformer tubes, caused by the flames used to provide the heat needed in conventional reforming, can be avoided. A recent study indicated that SMR + CLC may even reach higher efficiency and lower cost than conventional SMR and, thus, negative CO_2 capture cost.[110] Furthermore, 100% of CO_2 can be captured; NO_x can be avoided; and the absence of fuel ash may open for use of more expensive oxygen carriers.

Except for locating the steam reformer tubes in a FBHE, the reforming process is identical with conventional SMR. Thus,

https://doi.org/10.1021/acs.energyfuels.1c03615
Energy Fuels 2022, 36, 9588−9615

the gas from the steam reformer is led to a WGS reactor, where steam and CO react to increase the fraction of H_2 and CO_2, and further to pressure swing adsorption (PSA) to generate pure H_2 and an off-gas with combustibles that are used to provide the heat for the endothermic reforming. The steam reformer tubes will experience a much more benign environment, but the orientation would likely need to be changed from vertical to horizontal. The catalyst in the horizontal tubes can be expected to settle a bit, which could give a narrow path on the top of the inner cross section, where a part of the reacting gases could bypass the catalyst and compromise the performance of the tubes. A possible solution would be to insert a helix-shaped screw that forces the gas stream to move in a spiral through the tube (Figure 8).

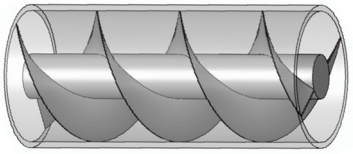

Figure 8. Illustration of a helix-shaped screw to move gas in a horizontal SMR tube.

4. NEEDED CIRCULATION

In comparison to other combustion technologies, CLC has two unique elements that are fundamental for the operation. The first is the oxygen carrier that needs to be able to perform its duty of transferring oxygen under the conditions prevailing in the reactor system. The second is that the circulation of the oxygen carrier needs to be sufficient to transfer necessary heat and oxygen to the FR.

Here, the transfer of sufficient heat is based on the assumption that the temperature difference between the AR and FR should be less than 50 °C. For ilmenite and coal, this gives a needed circulation of the oxygen carrier of 5.3 kg/s, MW_{th}, i.e., 1.06 tonne/s for 200 MW_{th}.[33] The heat loss in the FR because of the reaction between fuel and oxygen carrier is

$$\Delta H_{FR,O_2} = H_{i,O_2} - H_{OC,O_2} \quad (4)$$

where H_{i,O_2} is the lower heating value of the fuel per mole of oxygen and H_{OC,O_2} is the lower heating value of the oxygen carrier per mole of oxygen. Normally but dependent upon the oxygen carrier and fuel, more heat is released when oxygen reacts with the oxygen carrier than with the fuel, which means more heat is released in the AR compared to normal combustion. This is compensated by the endothermic reaction in the FR, which in practice means that the extra heat produced in the AR needs to be transferred to the FR. A convenient way to express the heat required in the FR is to express the heat loss related to the heating value of the fuel

$$F_H = \frac{\Delta H_{FR,O_2}}{H_{i,O_2}} \quad (5)$$

The loss in heat of reaction for ilmenite depends upon the phase separation of iron and titanium oxides. It is well-known that external layers of iron oxide are formed on the surface of ilmenite. The heat loss, F_H, for pure ilmenite is 12.8%, which means that the needed circulation is less than it is for iron oxide, having a heat loss of 18.2%. The value used for ilmenite is 15.5%, as determined from a sample that had experienced 88 h of pilot operation, and it also happens to be the average of the value for iron oxide and pure ilmenite.[112]

The effect of the oxygen carrier on the needed circulation is given in Table 4. Here, manganese and iron are assumed to be pure Mn_3O_4 and Fe_2O_3. In addition to the heat of reaction, the table also includes other estimated heat losses in the FR, with data from ref 33. Heating of fuel is two-thirds of the loss, while heating of fluidizing gas is one-third, and heat losses through reactor walls are a few percent. Manganese has a less endothermic reaction compared to ilmenite, leading to a reduction in needed circulation. Impurities in manganese ores, like silica, iron, and calcium, that form combined manganese oxides, would lead to further reduction in needed circulation because these combined manganese oxides give a positive reaction enthalpy in the FR.[31] For iron ore, the heat loss in the FR is larger than that of ilmenite, leading to a need for higher circulation.

Table 4. Needed Circulation Relative to Ilmenite for Fulfilling the Heat Balance[a]

	ilmenite	Mn ore	iron ore	$CaMnO_3$
loss of heat of reaction, F_H (%)	15.5	10.8	18.2	−19.8
other losses (%)	8.6	8.6	8.6	8.6
total heat loss in FR (%)	24.1	19.4	26.8	−11.2
needed increase in circulation as a result of heat losses relative to ilmenite (%)	ref	−20	11	not applicable[b]
heat capacity (J kg^{-1} K^{-1})	919.5	894.8	887.6	
needed increase in circulation as a result of heat capacity (%)	reference	3	3	
net needed increase in circulation relative to ilmenite (%)	reference	−17	15	not applicable[b]
mass-based oxygen transfer capacity (%)	1.7−5.0	7.0	3.3	4.5[c]

[a]Loss in heat of reaction in the FR is in a percentage of heat released from fuel in normal combustion, i.e., thermal power, with data from refs 30 and 31. [b]Exothermic reaction in the FR. [c]From $CaMnO_{2.92}$ to $CaMnO_{2.52}$.

For calcium manganate, $CaMnO_3$, the heat of reaction is exothermic in the FR; therefore, it would be possible to have a higher temperature in the FR, which is highly beneficial for the oxygen release.

Also shown in Table 4, is the maximum oxygen transfer of the oxygen carriers based on their fully oxidized state. Again, the ores are assumed to be pure, i.e., Mn_3O_4 and Fe_2O_3. The oxygen transfer capacity of the mineral ilmenite, $FeTiO_3$, ranges from that of pure oxidized ilmenite $Fe_2TiO_5 + TiO_2$ to that of fully phase-separated iron and titanium oxide $Fe_2O_3 + 2TiO_2$. The transfer capacity of calcium manganate is from $CaMnO_{2.92}$ to $CaMnO_{2.5}$.[31]

The heat balance also depends upon the fuel, although the heat per mole of oxygen is rather similar for most hydrocarbon-based fuels. As seen in Table 5, the heat of reaction of the fuels is, in all cases, lower than that with ilmenite, per mole of oxygen. Woody biomass and methane have a slightly lower heat of reaction, per mole of oxygen, than coal, which increases the heat loss in the FR reaction slightly. Moreover, the heating of the fuel, included under other losses, is higher for woody

https://doi.org/10.1021/acs.energyfuels.1c03615
Energy Fuels 2022, 36, 9588−9615

Table 5. Effect of Fuel on Needed Circulation[a]

	coal	wood	methane
heat of reaction per mole of O_2 (kJ/mol)	405.1	402.0	400.9
heat of reaction of ilmenite per mole of O_2 (kJ/mol)	468	468	468
heat loss in reaction, F_H (%)	15.5	16.4	16.7
other heat losses (%)	8.6	12.6	10.5
total heat losses (%)	24.1	29.0	27.2
needed increase in circulation relative to coal (%)	reference	20	13

[a]Data for dry fuels.

biomass than for coal. Thus, an increased circulation of the oxygen carrier is needed for these fuels (Table 5).

Furthermore, a high moisture content, which is common for biomass, will have a strong negative effect on the heating value, as seen in Table 6. First, the reaction enthalpy per mole of oxygen falls because of vaporization of steam, leading to a higher loss in the heat of reaction. Additionally, the steam produced by the moisture is heated to the reaction temperature. Finally, the lower reaction enthalpy also increases the flow of dry fuel for a given fuel power, which increases other losses somewhat. As seen, the need for higher circulation strongly depends upon the moisture content. Thus, a moisture content of 30% almost doubles the needed circulation relative to coal. In conclusion, there is a good reason to dry the fuels to be used in CLC.

Table 6. Effect of the Moisture Content for Woody Biomass

moisture (%)	0	20	30	50
heat of reaction with biomass per mole of O_2 (kJ/mol)	402	387.5	363.5	311.0
heat of reaction of ilmenite per mole of O_2 (kJ/mol)	468	468	468	468
heat loss in reaction (%)	16.4	20.8	28.8	50.5
heating steam from moisture (%)		3.0	5.2	13.4
other losses (%)	12.6	12.7	12.9	13.3
total losses (%)	29.0	36.5	46.8	77.1
needed increase in circulation relative to dry biomass (%)	reference	26	61	166
needed increase relative to coal (%)	20	51	94	220

The negative effect of moisture makes it reasonable to assume that the fuel will be dried to below 20% moisture. Thus, we can assume that the needed circulation for biomass is 8 kg MW^{-1} s^{-1} or 1.6 t/s for 200 MW.

The needed oxygen transfer is 15.7 kg/s for 200 MW. Thus, for a circulation of 1.6 t/s, oxygen transferred would be approximately 1% of the total mass circulated, which corresponds to a mass-based oxygen carrier conversion of 1%. The theoretical transfer capacities of the oxygen carriers are higher than that in all cases (Table 4). Reactivity investigations also confirm that actual oxygen transfer capacities of relevant oxygen carrier materials are well above 1%. Thus, it can be concluded that the minimum circulation is given by the heat balance. Obviously, this does not apply to calcium manganate, where the reactions in the FR are exothermic and only the oxygen transfer determines the needed circulation.

It may be an advantage for the integrity of the oxygen carrier to be only moderately converted in each cycle. There is little operational data available to support this, albeit data from 55 h of operation with a manganese ore indicate a negative effect of higher cyclic conversion.[42] However, the effect of cyclic conversion on formation of fines most likely differs between oxygen carriers.

5. ACTUAL CIRCULATION IN GASIFIERS AND CIRCULATING FLUIDIZED BED BOILER

5.1. Dual Fluidized Bed Gasifier. As noted above, a number of oxygen carriers have been shown to have the needed qualifications during a total of 12 000 h of operation in small-scale pilots. However, there is no industrial-scale operation demonstrating adequate circulation in extended operation of CLC. That said, sufficient circulation has been

Table 7. Composition and Heating Value of Volatiles[a]

		mol/kg of fuel	molar mass (g/mol)	g/kg of fuel	H_i (kJ/kmol of compound)	O_2 ratio	H_i (kJ/kg of fuel)	mol of O_2/kg of fuel	H_i (kJ/mol of O_2)
gases	CO	12.59	28.00	352.42	283.0	0.5	3.5621	6.293	566.0
	H_2	10.34	2.02	20.85	241.6	0.5	2.4997	5.172	483.3
	CH_4	4.57	16.03	73.25	802.7	2	3.6675	9.138	401.3
	C_2H_2	0.12	26.02	3.01	1253.8	2.5	0.1453	0.290	501.5
	C_2H_4	1.13	28.03	31.67	1323.1	3	1.4946	3.389	441.0
	C_2H_6	0.17	30.05	4.97	1428.8	3.5	0.2365	0.579	408.2
	C_3H_6	0.07	42.05	3.13	1925.8	4.5	0.1434	0.335	427.9
					sum of gases		11.7491	25.197	466.3

tars									
group	assumed compound	g/kg of fuel	molar mass (g/mol)	mol/kg	H_i (kJ/kg of compound)	O_2 ratio	H_i (kJ/kg of fuel)	mol of O_2/kg of fuel	H_i (kJ/mol of O_2)
1 (benzene)	benzene	19.28	78.05	0.247	40.1	7.5	0.7732	1.853	417.3
2 (1 ring)	cyclobutane	9.93	56.07	0.177	45.7	6	0.4537	1.062	427.0
3 (naphtalene)	naphtalene	5.76	128.07	0.045	38.8	12	0.2235	0.539	414.4
4 (2 ring)	cyclohexane	6.47	84.10	0.077	43.4	9	0.2807	0.693	405.2
5 (3 ring)	cyclohexane	8.13	84.10	0.097	43.4	9	0.3525	0.870	405.2
6 (phenolic species)	phenol	3.31	94.05	0.035	31.0	7	0.1026	0.246	416.7
					sum of tars	0	2.1862	5.263	415.4
					total	0	13.94	30.46	457.5

[a]The lower heating value is denoted H_i. The measured composition is given in column 3.

https://doi.org/10.1021/acs.energyfuels.1c03615
Energy Fuels 2022, 36, 9588−9615

Table 8. Heating Value of Potential Volatile Compounds per Mole of Oxygen

		H_i (kJ/mol of O_2)			H_i (kJ/mol of O_2)
propane	C_3H_8	408.7	toluene	C_7H_8	419.1
n-butane	C_3H_{10}	408.9	acetaldehyde	C_2H_4O	430.6
isobutane	C_3H_{10}	407.6	acetonitrile	C_2H_3N	431.9
n-pentane	C_3H_{12}	409.0	ammonia	NH_3	420.5
isopentane	C_3H_{12}	408.1	cumene	C_9H_{12}	412.8
neopentane	C_3H_{12}	407.4	cyclobutene	C_4H_6	445.6
n-hexane	C_6H_{14}	409.2	cyclopentane	C_5H_{10}	408.5
n-heptane	C_3H_{16}	409.2	cyclopropane	C_3H_6	434.2
n-octane	C_3H_{18}	409.3	hydrogen cyanide	CHN	519.3
n-nonane	C_9H_{20}	409.4	methyl *tert*-butyl ether	$C_5H_{12}O$	412.8
n-decane	$C_{10}H_{22}$	409.4	1-pentanol	$C_5H_{12}O$	407.8
butylene	C_3H_3	421.6	phenanthrene	$C_{14}H_{10}$	413.6
benzene	C_6H_6	422.6	2-propanol	C_3H_8O	405.4

shown in thermal gasification using dual fluidized beds: Güssing and Oberwart in Austria, Senden in Germany, Villach in France, and Gobigas in Sweden.[113,114] The latter has a fuel power of 32 MW, while the others are 8−15 MW. The gasification plants are built in the same way as most CLC pilots, i.e., as dual fludized beds with the combustion air driving the circulation to the gasifier/FR, where fuel is added. The key differences are that thermal gasification does not use oxygen carriers and that much more fuel is added relative to the air flow. This is because the purpose of gasification is to retain as much as possible of the fuel heating value in the gases produced and, thus, minimize the combustion air needed to supply the necessary heat for gasification. Consequently, the air flow in gasification is around a third of the air flow in combustion, for a given fuel addition. Thus, if used for CLC, the Gobigas plant would have a fuel power of around 10 MW, whereas the other four would correspond to CLCs of a size of 3−5 MW.

To compare gasification with chemical looping, the heat released by reaction of the volatiles with the oxygen carrier can be used. If the heat of reaction of the volatiles with oxygen is higher than the heat of reaction of ilmenite with oxygen, this means that the reaction of volatiles with ilmenite in the FR is exothermic and vice versa. Further, if the reaction of volatiles with ilmenite is exothermic, it means that the heat balance of the gasifier/FR is improved by the presence of ilmenite. Thus

$$\Delta H_{\text{ilm-gg}} = \Delta H_{\text{O}_2\text{-gg}} - \Delta H_{\text{ilm-O}_2} \quad (6)$$

where $\Delta H_{\text{ilm-gg}}$ is the reaction enthalpy for reaction of ilmenite with gasification gas, $\Delta H_{\text{ilm-O}_2}$ is the reaction enthalpy for ilmenite with oxygen, and $\Delta H_{\text{O}_2\text{-gg}}$ is the reaction enthalpy for oxygen with gasification gas. Thus, if $\Delta H_{\text{ilm-gg}}$ is exothermic, gasification needs more energy to be transferred to the FR compared to chemical looping for the same amount of fuel.

To assess whether the overall reaction of volatiles with ilmenite is exothermic, measured gas composition from a gasifier can be used. Table 7 shows data from a 12 MW CFB equipped with a thermal gasifier.[57] Gases are presented in moles per kilogram of fuel, whereas tar is presented in grams per kilogram of fuel. From the molar mass and heating value, the heat release per kilogram of fuel and the oxygen consumption per kilogram of fuel can be derived. Summarizing the heat produced and oxygen consumed and taking the ratio of these sums yield the heat release for burning the volatiles per mole of oxygen. As seen, the heat release of the gases, 466 kg/mol of O_2 is almost identical to the heat of reaction with ilmenite, 468 kJ/mol of O_2, whereas it is estimated at 415 kJ/mol of O_2 for the tars. For the tars, one compound was selected to represent each of the six groups of tars. On the basis of the small differences between hydrocarbons, the error from choosing one compound to represent the group should be small. This is illustrated by Table 8, which shows that the majority of the hydrocarbons deviate from 415 kJ/mol by a few percent. Moreover, the heating value and oxygen consumption are dominated by the gases. Adding up the contribution from gases and tars (Table 9), it is seen that the heat of reaction of the volatiles with oxygen is 457 kg/mol of O_2, which is 98% of the value for the reaction with ilmenite. The difference is within the range of uncertainty of the measured gas composition.

Table 9. Heat Balance for Gasification Relative to Chemical Looping

	reaction	kJ/mol of O_2
$\Delta H_{\text{ilm-O}_2}$	ilmenite with oxygen	468
$\Delta H_{\text{O}_2\text{-gg}}$	oxygen with gasification gas	457.5
$\Delta H_{\text{ilm-gg}}$	ilmenite with gasification gas	−10.5

In conclusion, the heat needed in the FR/gasifier is essentially equal for chemical looping and gasification per unit of fuel. However, the fuel addition to the FR/gasifier is typically 3 times higher for gasification compared to chemical looping if related to the air addition to the riser/AR. The riser and air flow of the riser drive the circulation; therefore, for a similar riser and air flow, gasification will use 3 times more fuel. Consequently, the heat needed for heating and devolatilization of fuel will be 3 times higher in gasification. Hence, there is little doubt that, if the circulation in a gasifier is sufficiently high to give a reasonable temperature in the FR, the circulation would also be sufficient for CLC. Thus, it can be safely concluded that there is experience from biomass gasifiers giving proof of concept for a dual fluidized bed in CLC, in the size range up to 10 MW.

5.2. Circulating Fluidized Bed Boilers. Because of the similarities, it is relevant to consider experiences from CFB boilers. However, circulation data for large-scale CFB boilers are difficult to come by because there is no easy way to measure the circulation. However, the pressure drop in the uppermost part of the riser can be used to estimate the solids

https://doi.org/10.1021/acs.energyfuels.1c03615
Energy Fuels 2022, 36, 9588−9615

concentration, and from this, the upward flow in the riser, G_s, can be derived

$$G_s = \rho_s(u_0 - u_s) \quad (7)$$

where ρ_s is the solids concentration (kg/m^3), u_0 is the gas velocity, and u_s is the slip velocity, i.e., the downward velocity of particles. Here, it assumed that the transported particles behave as individual particles; therefore, the slip velocity is equal to the terminal velocity, u_t, i.e., the calculated free fall velocity of a particle of a given size and density. The particles have a size distribution, which is different in the top of a riser compared to the bottom bed. The estimation of u_t is based on d_{50}; that is, half of the particle mass is below this diameter. Examples of terminal velocities are given in Table 10 for materials used in CFB boilers and CLC. The first three are the those used in operation of a 12 MW CFB boiler to be discussed below and shown in Figure 9. The following three values are from commercial CFB boilers, all with a thermal power of 235 MW or higher, and finally two materials used in chemical looping pilot operation are included.

Table 10. Terminal Velocities of Some Typical Bed Materials

	average size (mm)	particle density (kg/m^3)	terminal velocity (m/s)
silica sand	0.2	2600	1.0[116]
silica sand	0.32	2600	2.1[116]
silica sand	0.44	2600	3.3[116]
Emile Huchet[117]	0.25	2600	1.5
Zibo[117]	0.3	2600	1.9
Turow[117]	0.3	2600	1.9
ilmenite[118]	0.17	3600	0.85
Mn ore[118]	0.14	3200	0.62

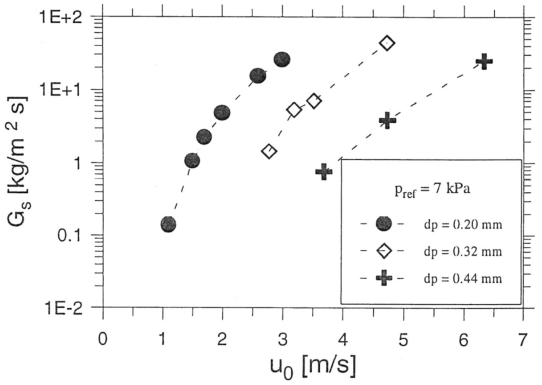

Figure 9. Upward flow on the top of a 12 MW$_{th}$ CFB. This figure was reproduced with permission from ref 116. Copyright 1995 American Society of Mechanical Engineers (ASME).

The terminal velocity is well below the actual velocity used in commercial CFB boilers. Thus, if the particles would behave as individual particles, they would immediately be entrained by the gas, causing the bed to disappear. Nevertheless, a dense bed forms in the bottom zone. The bed is characterized by a high through flow of gas that bypasses the bed in bubbles at high gas velocity.[115] Consequently, the particles inside the dense phase are not subject to the high velocities and, therefore, not readily entrained. Instead, particles are thrown up by bubbles erupting at the surface of the dense bed, creating a splash zone above the bed. Here, particles may appear in clusters or aggregates that increase the falling velocity, which allows them to fall back onto the bed. A part of the particles, however, is entrained by the gas in an upward flow that decreases with height. This decrease means that there is a significant downward flow of particles. It is well-known that there is a large downward flow along the walls where the gas velocity is lower and, more importantly, the particles concentrate to form a wall layer of descending particles. A downward flow can also be caused by particles interacting in the core region to form particle aggregates, clusters, that fall downward. Leckner argued that solids clustering in the core region is small because of the low particle concentration.[115] However, the extent to which clusters form in the core region in large boilers needs to be further studied.

For a lack of data, the circulation has often been assumed to be equal to the particle flux, G_s, on the top. However, all of the particles that reach the top of the riser may not continue to the cyclone. This relationship between the upward flow on the top of the riser, $G_{s,top}$, and the actual circulation via the cyclone, G_s*, can be expressed as

$$G_s^* = G_{s,top}(1 - k_b) \quad (8)$$

where k_b is the backflow ratio. Assuming a cross section in the AR of 0.2 m^2/MW and a needed circulation of 1.6 t/s, the needed circulation per unit of riser cross section, G_s*, is 40 kg m^{-2} s^{-1}.

According to Yue et al.,[119] the circulation in large CFB boilers from major boiler manufacturers is around 6−10 kg m^{-2} s^{-1} at fluidizing velocities in the range of 5−6 m/s. It is not clear how these flows were determined, except that data were by "estimation or field measurements". Wu et al. reported that the circulation in a 300 MW$_e$ CFB boiler operated at 5.4 m/s was 42 kg m^{-2} s^{-1}.[120] However, here, pressure drop measurements were used; therefore, the circulation measured is $G_{s,top}$ rather than G_s*.

With a population balance model and known outgoing flows and particle size distributions, the circulation in a 75 MW$_{th}$ CFB burning refuse-derived fuel (RDF) was estimated to 1343 t/h, corresponding to 5 kg MW^{-1} s^{-1}.[121] A similar modeling approach was used to estimate the circulation in a coal-fired 996 MW$_{th}$ CFB in Tauron,[122] giving a circulation of 23−26 kg m^{-2} s^{-1}.[123] Li et al. used the temperature difference over external Intrex fluidized bed heat exchangers combined with temperature measurements, giving the ratio of internal and external circulation flows, to estimate the circulation flow through four of the total eight cyclones of a 550 MW$_e$ CFB boiler.[124] The average flow through these was 464 kg/s, corresponding to 3 kg MW^{-1} s^{-1}.[125] If the data from Wu et al. based on pressure drops are excluded, the estimated circulation in the boilers is in the range of 15−60% of the needed flow.

The possibility to increase the circulation with increased velocity is limited, because it is well-known that erosion of boiler tube walls increases with velocity. According to Yue et al.,[119] severe erosion can be expected above 6 m/s and commercial CFB boilers often operate close to this limit, i.e., 5−6 m/s.

Johnsson and Leckner[116] presented circulation data or rather the upward flow on the top from a 12 MW$_{th}$ CFB with particle sizes of 0.2, 0.32, and 0.44 mm and gas velocities ranging from 1 to 6 m/s (Figure 9). The velocity was raised with the particle size, and for each particle size, the velocity was varied in an

https://doi.org/10.1021/acs.energyfuels.1c03615
Energy Fuels 2022, 36, 9588−9615

interval of around 2 m/s. k_b was assumed to be zero, and circulation ranged between 0.1 and 30 kg m^{-2} s^{-1}.

Later, the external circulation was measured in the same boiler using the heat balance over the fluidized bed heat exchanger cooling the material from the cyclone.[126] With a particle size of 0.3 mm and a top velocity of 4.5 m/s, the highest circulation of 3.7 kg m^{-2} s^{-1} was reached (Figure 10).

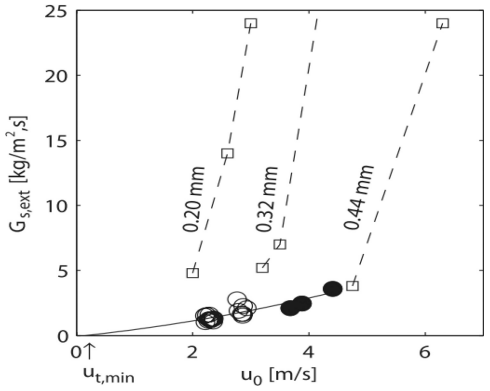

Figure 10. Actual circulation measured by heat balance[126] (filled and open circles). Boxes and dashed lines show the upward flow from Figure 9. This figure was reproduced with permission from the authors and the editor of ref 126. No copyright was claimed in the publication.

This can be compared to the data in Figure 9 that shows an upward solids flow on the top of almost 10 times higher, 30 kg m^{-2} s^{-1}, for similar conditions, i.e., 0.32 mm particle size and top velocity of 4.7 m/s. In both cases, the total pressure drop was 7 kPa and no secondary air was used. The data in Figure 10 were obtained with several fuels, with ashes resulting in different particle size distributions. The study found no significant effect of the primary air fraction. A test where solids inventory was increased to raise the pressure drop above 9 kPa showed no effect on circulation. These data indicate a high backflow on the top with a k_b value of almost 90%.

However, *in situ* measurements of the flux profile in the same boiler found a lower backflow, with a k_b value of 0.61.[127] Furthermore, a $^1/_9$ scaled cold-flow model of the same boiler compared measured circulation, using a butterfly valve, and calculated circulation, i.e., from pressure drop measurements, and found measured circulation to be 40% lower, that is, a backflow of 40%.[128] Johansson et al., on the other hand, reported a backflow of only 2−14% for five CFB boilers in the range from 72 MW_{th} to 235 MW_e, with 12% for the 12 MW CFB discussed above.[129]

In contrast to CLC, where a sufficient circulation is mandatory, a raised backflow would often be an advantage in a CFB. Johnsson et al.[128] investigated 12 different configurations of the riser top, with the purpose of affecting the backflow, and found a variation of more than 1 order of magnitude in the circulation flow.

Literature data from cold-flow models clearly indicate that a significant fraction of the upward flow can be retained on the top, where the gas particle mixture enters the cyclone. Djerf et al. investigated circulation in a cold-flow model of a 200 MW CFB and found the value of k_b to vary in the range of 0−0.82.[130] The data indicate no backflow at low gas velocities and low upward flow. $G_{s,top}$ rises from 0 up to 15 kg m^{-2} s^{-1} when gas velocity is increased, whereas G_s* first increases to around 2 kg m^{-2} s^{-1} and then seems to remain at this level independent of the gas velocity, cf. Figure 11. The increased

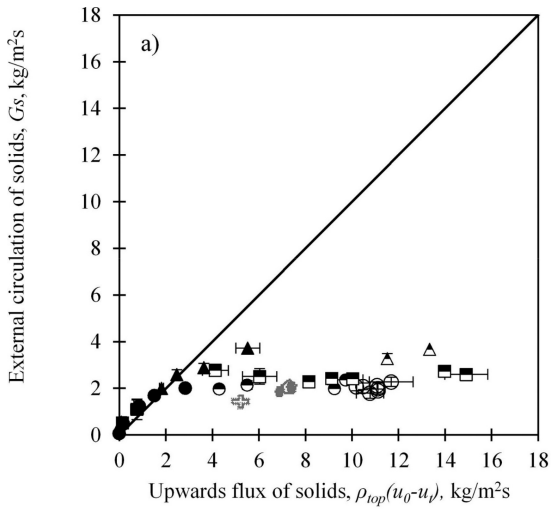

Figure 11. Measured external circulation versus upward solids flux on the top of a cold-flow model of a 200 MW_{th} CFB. This figure was reproduced with permission from ref 130. Copyright 2020 the authors.

backflow ratio at higher gas velocities was correlated to the Stokes number, which describes the unwillingness of particles to follow a fluid. In other words, coarser bed particles reach the top because of reduced particle segregation, and these coarser particles do not follow the gas stream into the cyclone. Djerf et al. conclude that this result "raises questions as to the validity of an approximation that appears commonly in the literature, estimating the solids circulation from the solids concentration in the upper part of the riser... with the single particle velocity $(u_g - u_t)$, i.e., disregarding the back-flow effect".

Because the gas velocity is much higher than the fall velocity of single particles, there are two mechanisms that can give a downward flow, i.e., the formation of particle clusters or particles reaching the wall, where velocity is low, or a combination of these. Cluster formation would obviously be more likely at a higher concentration of particles: therefore, it is not so surprising if k_b is low when particles are diluted and rises with an increasing concentration on the top.

Markström and Lyngfelt found that the external circulation was 29% of the upward flow on the top of a scaled model of a 100 kW CLC reactor;[131] albeit, the ratio was higher at a lower circulation. Linderholm et al. found an external circulation, which was 7−10% of the upward flow in a 100 kW CLC, with the lower numbers found at higher flows.[132]

Despite the fact that sufficient circulation is crucial for CLC to work, the chemical looping literature has given little consideration to the challenge of securing adequate circulation in the industrial scale. It is clear, however, that a design where the AR is a riser driving the circulation similar to a CFB is normally assumed for the full scale. Lyngfelt et al. did the first estimations of the viability of a CLC system of interconnected fluidized beds and concluded that the needed circulation flows were feasible.[133] However, this was based on the results shown in Figure 9 that overestimated the circulation, as discussed above.

Marx et al.[134] proposed a design for a 10 MW CLC pilot, where they stated that the riser velocity range "for proper

https://doi.org/10.1021/acs.energyfuels.1c03615
Energy Fuels 2022, 36, 9588−9615

operation" was 7−8 m/s or 1.2 times the velocity, where "significant solids entrainment... is observed" according to Bi and Grace.[135]

Abad et al.[136] proposed a 100 MW_{th} CLC boiler with a cross section of 25 m^2 and an estimated needed circulation of 820 kg/s, leading to a needed circulation flow of 32 kg m^{-2} s^{-1}. According to the paper, this circulation flow "may be easily reached under these conditions". The bottom velocity was 6 m/s, but the consumption of oxygen by the oxygen carrier, which is expected to take place mainly in the lower part, will lower the velocity below 5 m/s. The material used for the design was ilmenite and reported to have a terminal velocity of 1 m/s.

Sharma et al.[137] presented a design for a 200 MW methane-fired CLC boiler, with a circulation rate of 3780 kg/s, but had no discussion how to reach this circulation.

Lyngfelt and Leckner[33] were more concerned about reaching adequate circulation in their design of a 1000 MW_{th} solid fuel CLC and assumed that circulation would need to increase by a factor of 4 compared to a reference CFB based on the previously cited data from Yue et al. and Wu et al. They assumed this increase could be accomplished by lowering the riser height by 15 m and reducing the particle size by 10%.[33]

Examples of measured solids concentrations in two CFB boilers with a thermal power of 109 and 226 MW are given in Figure 12. The fluidization velocities in these are 5.3 and 6.3

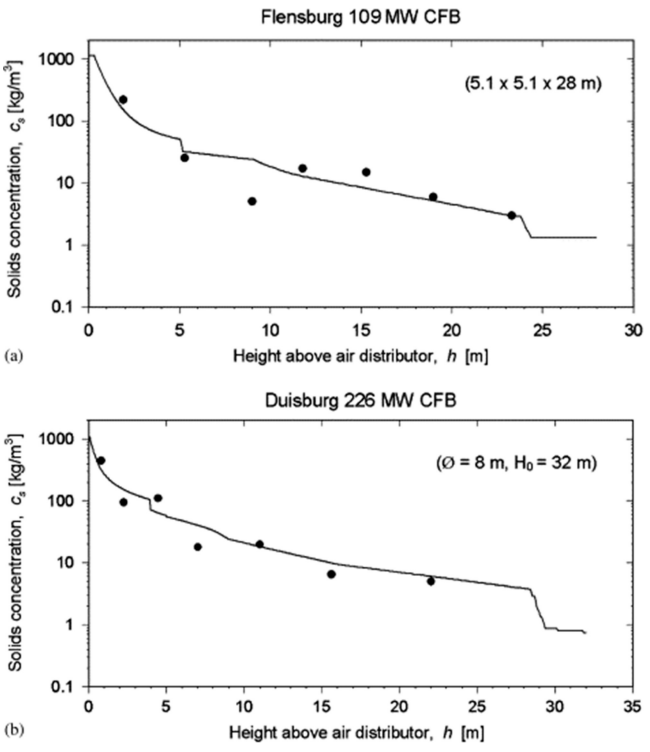

Figure 12. Experimental data from two CFB boilers,[138] adapted from ref 139. This figure was reproduced with permission from ref 138. Copyright 2006 Elsevier.

m/s. With the assumption that $u_0 - u_s$ is 5 m/s, the upward flow G_s is obtained from multiplying the solids concentration in Figure 12 by 5, cf. eq 7. Thus, a needed circulation of 40 kg m^{-2} s^{-1} would correspond to a density of 8 kg/m^3. The data in Figure 12 suggest that the solids density is higher than 10 kg/m^3 up to around 15 m height but falls below that level as height increases. Further accounting for backflow on the top, it is clear that these CFB boilers have a circulation far below what is needed in CLC.

Similar data from the three CFB boilers Emile Huchet 125 MW_e, Zibo 135 MW_e, and Turow 235 MW_{th} are shown in Figure 13. With the assumption that k_b was 0.8, Djerf

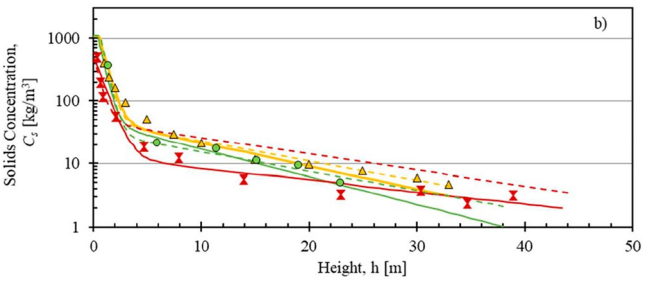

Figure 13. Solids concentration versus height:[117] (yellow triangles) Emile Huchet, (green circles) Zibo, and (red hourglasses) Turow. This figure was reproduced with permission from ref 117. Copyright 2021 the author.

estimated the external circulation of the Emile Huchet and Zibo CFBs to be around 0.2−0.3 kg MW^{-1} s^{-1}, i.e., around 5% of circulation needed for CLC. The solids circulation is likely not higher for the Turow CFB boiler, judging from the solids concentrations shown in Figure 13.

The downflow at the wall was measured at 12.5 m height in the 250 MW_e Gardanne CFB boiler, using a 1.5 × 1.5 m box at the wall that led collected material to the outside. It was found to be 100−150 t/h, which translates to a downflow of 1.6−2.5 kg MW^{-1} s^{-1}, a bit below the needed 8 kg MW^{-1} s^{-1}.[140] The downflow was also verified by probe measurements, giving similar results. However, probe measurements at the 125 MW_e Emile Huchet CFB boiler, at a height of 10.8 m, showed a downflow along the walls, which was 2.7−7 times higher than that in Gardanne,[140] where the lower number is closest to the wall and should be most relevant. This translates to a downflow of 5−8 kg MW^{-1} s^{-1}. This is also consistent with the solids concentration of 20 kg/m^3 at this height (Figure 13), which corresponds to an upward flow of 65 kg m^{-2} s^{-1} or 11 kg MW^{-1} s^{-1}. Furthermore, the slope in the solids concentration of the Emile Huchet boiler in Figure 13 shows a decrease with height of 8.2%/m in this region, which means that the upward flow should increase by 66% going from 11 to 5 m height, which would give a higher flow than what is needed. Thus, measurements of the downflow are consistent with the concentration measurements, and both indicate that the downflow is in the same order of magnitude as what is needed for CLC. Being in the right order of magnitude is not enough, however. Therefore, a careful control of the bed material size distribution is needed, as discussed in the following section.

5.3. Particle Size. From the previous section, it appears that the downflow along the walls can give adequate circulation. However, it is important to emphasize that the particle size provides a most powerful tool to control the circulation. On the basis of the data shown in Figure 9, it was estimated that an already 10% reduction in the particle diameter is sufficient to double the circulation.[33] The oxygen carrier materials typically used in CLC pilots are smaller and have lower terminal velocities (see Table 10) and would give much higher circulation, cf. Figure 9. An important difference between a CLC and a CFB boiler is therefore an imperative

https://doi.org/10.1021/acs.energyfuels.1c03615
Energy Fuels 2022, 36, 9588−9615

need to maintain the particle size distribution within the range that gives an adequate circulation. This will require a well-developed control of the addition of makeup material, e.g., by monitoring the temperature or riser pressure drops.

In CFB boiler operation, an increase in the particle size is caused by the fuel ash. In CLC, however, the optimum fuel size is smaller because of the need to gasify the char before it is transported to the AR by the material circulation. Thus, operation with coarse coal, <8 mm, gave a high loss of char to the AR in a 1 MW CLC,[141] whereas operation of the same unit with pulverized coal gave a large loss of char in the gas from the FR.[142] Likewise, operation of a 100 kW CLC with pulverized coal showed a high loss of char, whereas this loss was significantly reduced with coal particles in the size range of 90−300 μm, and the loss to the AR was still only 1%.[24] Clearly, the optimal size is well above that of pulverized coal but well below the "several millimeters" used in the 1 MW CLC pilot. Thus, the optimal size is probably similar to the size of the bed material. With such a fuel size and considering that the ash is only part of the fuel added, a greater portion of the ash would be elutriated and it is less likely that the ash would not contribute to coarsening of the bed material. The optimal size of woody fuels is not clear, but there are several aspects to consider when comparing to to coal, including higher costs of grinding, faster gasification, lower ash content, and less fixed carbon. Because of the lower ash and fixed carbon fractions, the fuel particles can also be expected to break more easily and form more fly ash compared to coal.

In view of the higher costs of an oxygen carrier compared to commonly used sand/limestone, magnetic separation of the oxygen carrier from the ash can be used to reduce costs.[58]

5.4. Summary. The data presented from large-scale CFB boilers are uncertain and differing, and there seems to be a large spread in the estimated backflow ratio, even for data relating to the same CFB boiler. The range of estimated circulation is 5−50% of what is needed for a CLC boiler, thus well below what is needed for CLC. Because of the risk for erosion of boiler tube walls, higher velocity is likely not a possible path for reaching the circulation needed. In contrast, Figure 9 shows the strong influence of the particle size on the upward flow. Extrapolation of the data for the lower particle sizes in Figure 9 to much higher velocities would give the needed circulation. This assumes that the backflow fraction, k_b, is not too large or increases too much with increased upward flow. A possible option to lower the backflow fraction, k_b, would be to design the top of the riser to promote solids to go to the cyclone inlet. There is nothing to indicate that it would not be possible to reach the adequate circulation in a CFB-type design. On the contrary, it is evident that it is possible to increase the circulation dramatically by reducing the particle size. However, there are good reasons to be cautious with such a strategy: (1) A design would not be based on existing operational experiences with the needed flows but rather on the extrapolation of results from actual operation, such as the data from the 12 MW_{th} CFB with a 13 m riser, which is well below the 30−50 m height of industrial-scale boilers. (2) It requires that the backflow ratio k_b is not too large. There is little experience of large-scale CFBs with tops aimed at preventing the backflow. (3) There is a significant risk that leading a much higher flow of solids into the cyclone would also lead to much higher loss of particles, in particular, as the increase in flow results from reducing the particle size. The higher loading and smaller particle size should lead to reduced separation efficiency, which, applied to a much higher flow of solids, can give a dramatic increase in particles escaping the cyclone with the gas flow. Possible countermeasures are a more efficient cyclone design and the addition of a second cyclone with material recycling, but these come with added costs and, in the second case, space requirements.

In short, decreasing the particle size and increasing the circulation by an order of magnitude or more, in comparison to existing CFB boilers, would mean designing an industrial-scale boiler for conditions outside the experience of today's CFB boilers. Although possible, it could be difficult to find design and operational conditions that secure adequate circulation and not without risks to rely on the AR riser as a safe way of providing adequate circulation in the industrial scale.

Assuming that attrition in the bottom region is limiting for the gas velocities in the riser/AR raises another complication for CLC. In normal combustion of solid fuels, there is an increase in gas flow because of combustion. This is around 3−15% for coal and woody biomass fuels on a dry basis and even higher for wet fuels. In a CLC AR, on the other hand, the oxygen consumption leads to a fall in gas flow of 18% at an air ratio of 1.2. This is because the combustion products, CO_2 and H_2O, are formed in the FR. Consequently, a CLC boiler will have 20−28% lower gas flow in the upper part of the riser for a similar load compared to a CFB boiler.

In normal CFB combustion, the velocities in the lower part are further lowered by adding part of the air as secondary air. On the other hand, some CFB boilers have sloping walls in the bottom zone that raise the velocity in this zone. Secondary air is not a good idea in CLC because there are no gaseous compounds or light elutriated char particles to burn in the riser. The air needs to react with the oxygen carrier, which is mainly present in the bottom zone.

Below, the possibility to reach adequate circulation by use of the downflow of particles along the walls is presented.

6. USE OF DOWNWARD WALL FLOW IN AN AIR REACTOR FOR CIRCULATION

As shown in Figures 12 and 13, there is an upward particle flow that falls rapidly with height. At lower heights, this upward flow is well in excess of the circulation flow needed. The decrease in upward flow with height means that there is a corresponding downward flow, which takes place along the walls, at least above the splash zone. With the neglect of any downflow in the core region, the wall downflow at any height should be equal to the upward flow minus the external circulation

$$G_{s,wall} = G_s - G_{s,top}(1 - k_b) \quad (9)$$

where $G_{s,wall}$ is the downflow along the walls per square meter of riser cross section. At lower heights, the downflow along the walls is approximately equal to the upward flow because external circulation is small in comparison.

Below, a design for a 200 MW_{th} CLC boiler is proposed. Noting that the air needed per thermal power is almost equal for the fuels coal, woody biomass, and methane/natural gas (Table 5), the design is relevant for all three of these fuels.

Generally, it would be an advantage to collect the downward wall flow as low as possible, where the flow is higher. At the same time, the driving force for leading the flow through the loop seals must be sufficient. In the design proposed below, the

https://doi.org/10.1021/acs.energyfuels.1c03615
Energy Fuels 2022, 36, 9588−9615

collection of material in the AR is performed at a height of 5.2−7.5 m.

7. 200 MW CLC−CFB DESIGN

The design of the proposed 200 MW_{th} CLC−CFB is based on the following premises: (1) Although there is a lot of experience from operating small CLC pilots, the proposed boiler would be a first of its kind, and unexpected difficulties may arise. Therefore, the design should have high flexibility, to ensure that the boiler can be used as a production unit. Thus, the design will have an AR that can also be used as a CFB boiler. (2) Furthermore, the unit should be designed to have good flexibility with respect to the fuel and oxygen carrier as well as other operational parameters, like the temperature, load, and solids inventory. This is to accommodate for unexpected difficulties but also to allow for using the boiler for the purpose of research and development, including evaluating different operational strategies, fuels, and oxygen carriers. (3) The unit should also be equipped with detailed pressure measurements and be fitted with ports for *in situ* gas and solids sampling and visual observation.

The general outline of the boiler is shown in Figure 14, with the AR and FR shown in blue and red in Figure 14. The riser

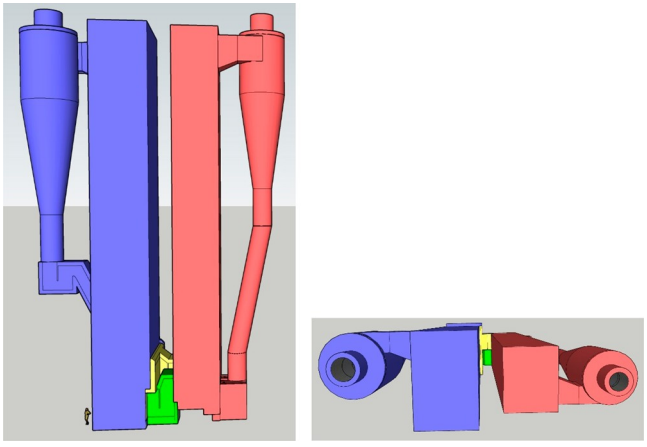

Figure 14. Outline of the 200 MW CLC boiler: (left) top view and (right) front view.

Table 11. Inner Dimensions of Risers

	air reactor	fuel reactor
height (m)	40	38.5
cross section (m^2)	5 × 8 = 40	4 × 5 = 20
cross section, lower part (m^2)	4.5 × 7.5 = 34	
thickness insulated wall (m)	0.4	0.4

dimensions are given in Table 11. The dimensions were chosen to give a gas velocity of 6 m/s of the AR not considering reactions and a velocity of 5.5 m/s in the upper part of the FR assuming full gas conversion, with biomass fuel with 20% moisture. The two reactors are connected through two loop seals, with the yellow leading the oxygen carrier from the AR to the FR and the green returning the oxygen carrier to the AR. To achieve high flexibility, a significant part of the cooling of the AR/CFB will use controllable external fluidized heat exchangers, not shown in the figure. There will also be two systems for feeding solid fuel, one for the FR and one for the AR/CFB. After the outlet of the FR, there will be a post-oxidation chamber, where combustibles remaining in the outlet gas can be oxidized by either oxygen or air.

Figure 15 shows the design proposal for collection of the wall downflow, henceforth termed "balconies", and loop seals for the transfer of the oxygen carrier between the reactors. To the left, the balconies collecting the downflow and the loop seal leading to the FR are shown, and on the right-hand side, the mirror image of the loop seal leading the return flow back to the AR is shown. The real positioning of the return flow is illustrated by the green dotted line in the figure. Three-dimensional (3D) views of the design are shown in Figure 16a for the section cut of the loop seal leading to the FR, Figure 16b for the section cut of the loop seal leading back to the AR, and Figure 17 for the top view section cut.

The dimensions are shown in Figure 15. Thus, the height at which the wall downflow is collected in the AR is 5.2 m above the bottom plate. The width of the loop seals is 2 m, while the aperture is 1 m, giving a 2 m^2 cross section for the critical horizontal transfer through the loop seal. With a flow of 1.5 t/s, this means a mass transfer of 0.75 t m^{-2} s^{-1}. For activated ilmenite with a particle density of 2800 kg/m^3 and a bulk density of 1600 kg/m^3[131] and assuming a bed expansion of 20%, the bed density is 1340 kg/m^3. Thus, the needed material velocity would be 0.56 m/s, which is not unreasonable. It is hard to find literature data on possible velocities, and available experimental work has been performed in small cold-flow models. Basu, however, suggests an interval of 0.05−0.25 m/s for the solids velocity, noting that the "deeper the loops seal and the greater its fluidizing velocity, the higher the allowable horizontal velocity".[143]

The height of both loop seals is 2.5 m on the inlet side and 1.5 m on the outlet side, providing 1 m of height to drive the solids flow through the loop seal. Likewise, the inlet and outlet of the FR differ by 1 m to safely move the material through the FR. To prevent the bed material flow from taking a short-cut, a wall is placed in the lower part of the FR extending to the center of the reactor. Finally, the flow is returned to the AR at a height of 1.5 m, which should be sufficient to be above the surface of the dense bottom bed. The horizontal cross sections leading through the loop seals are also 2 m^2 or more, corresponding to an upward/downward velocity of 0.46 m/s. This should be less critical than the vertical cross section below the aperture, and Basu states "one could choose" velocities "as less than 1.0 m/s".[143]

In addition to providing the paths of circulation, the loop seals also provide the necessary sealing that prevents mixing of gases between the reactors. Any leak through the loop seal would either mean CO_2 is lost for capture or that the CO_2/H_2O stream is diluted with nitrogen from the combustion air. A leak occurs if the pressure difference between the AR and the FR is too high, i.e., if the pressure difference over the loop seal $P_2 - P_1$ is greater than ρgh, where h is the difference in height from the overweir of the outlet and the underweir (see Figure 18). Thus, if the pressure of the FR increases compared to the AR, the bed surface of the inlet side of the loop seal leading from the FR will move downward, i.e., if we neglect the continuous addition of new material. If the density of the bed in the loop seal is 1340 kg/m^3, the pressure drop provided by the height of the column of the outlet side, which is 0.5 m, will be 6.7 kPa. If the overpressure in the FR exceeds 6.7 kPa, the bed surface falls to the level of the underweir and gas leaks into

https://doi.org/10.1021/acs.energyfuels.1c03615
Energy Fuels 2022, 36, 9588−9615

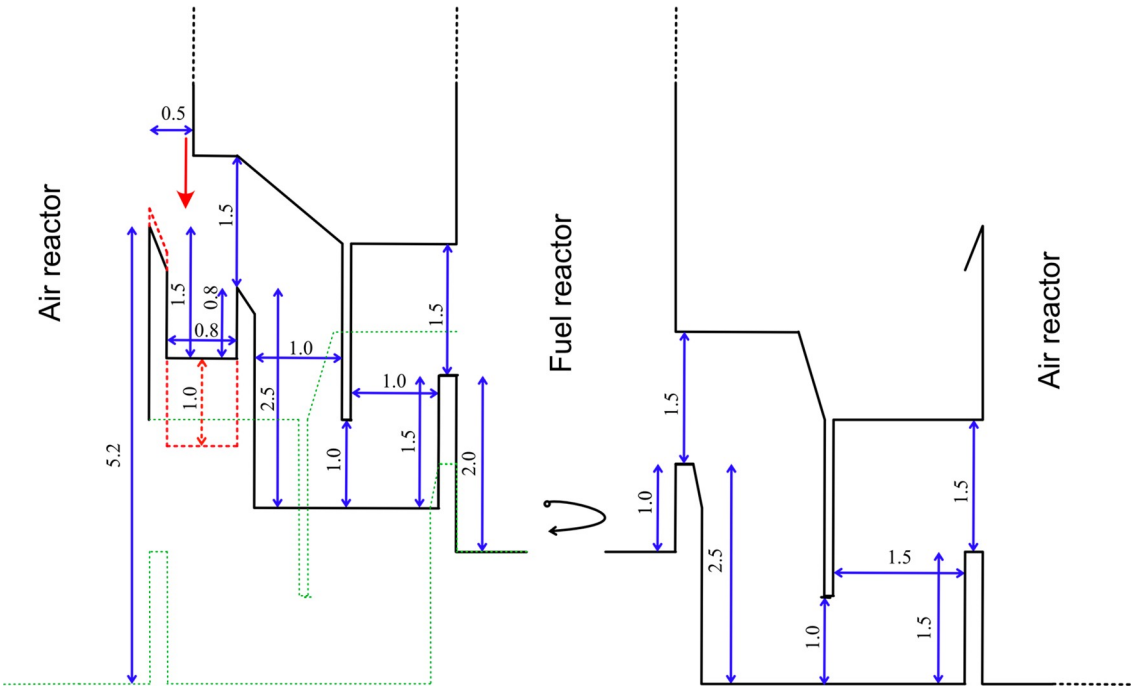

Figure 15. Loop seal leading the circulation from the AR to the FR (left) and back to the AR (green dotted lines, also shown in the mirror image to the right).

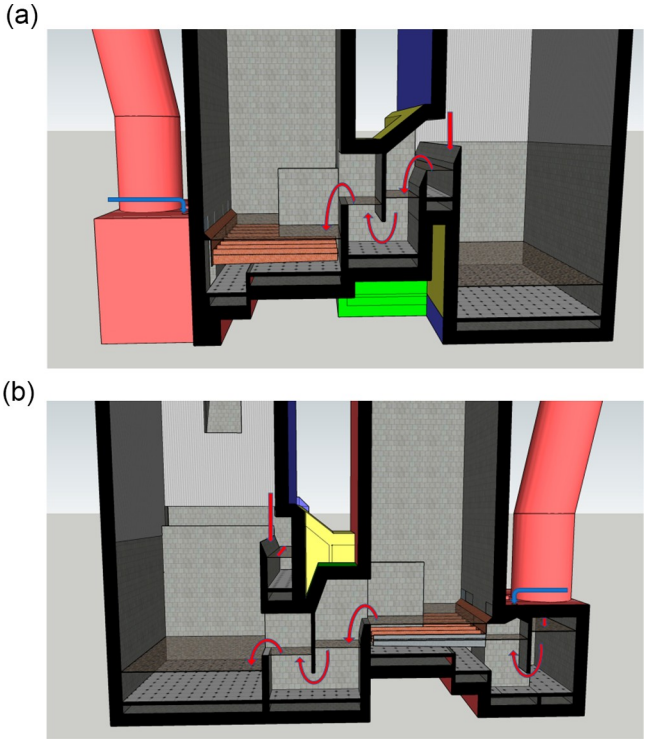

Figure 16. (a) Section cut of the loop seal leading from the AR (right) to the FR (left) seen from the rear side of the unit. The transparent surfaces suggest the height of the dense beds. The blue arrow shows where the fuel is to be added. The brown arms indicate the volatiles distributor. (b) Section cut of the loop seal leading back from the FR (right) to the AR (left) seen from the front side of the unit. The blue arrow shows where the fuel is to be added. The brown arms indicate the volatiles distributor.

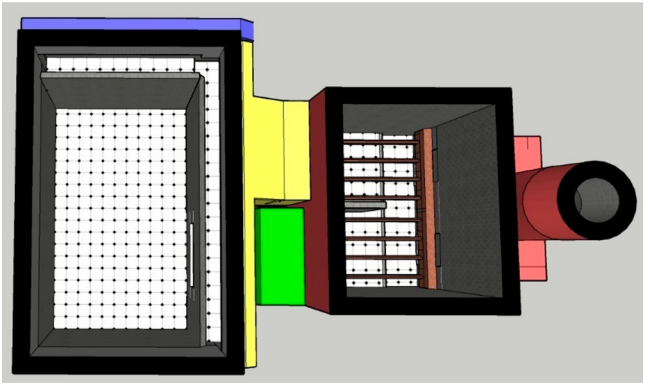

Figure 17. Top view section at approximately 7 m height.

the AR. Likewise, a similar overpressure in the AR will push down the bed level in the inlet of the loop seal, leading to the FR. Hence, the operation of such a system will require careful control of the pressures in the bottom part of the reactor system to ensure that there is no leakage.

Figures 15−17 illustrate the design of the balconies that collect the downflow. The depth of the balcony is restricted above the return channel (Figure 16b), but along the rest of the walls, it can be deeper to increase the cross section to facilitate the mass flow along the balcony channel. This is illustrated by the dashed red lines in Figure 15. With exception of the part of the channel above the return, the cross section is $2.5 \times 0.8 = 2\ m^2$. The maximum lateral flow, which is just where it reaches the section where the material is overflowing into the loop seal, should be about half of the total flow. Thus, the needed lateral velocity is around half of that in the loop seal aperture, which also has a cross section of $2\ m^2$.

To the right, Figure 16b shows the loop seal returning the internal circulation flow from the cyclone downcomer to the FR. Because of the pressure drop over the FR riser and inlet, the pressure will be lower in the downcomer. The bed surface of the particle column in the loop seal inlet will be higher than

https://doi.org/10.1021/acs.energyfuels.1c03615
Energy Fuels 2022, 36, 9588−9615

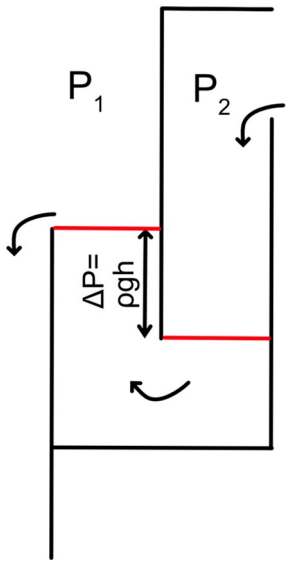

Figure 18. Illustration of the pressure difference needed to give a gas leak via the loop seal.

the bed surface in the FR, both to overcome the pressure difference and to provide the driving force for the movement of bed material through the seal. This flow of material will also pass below the fuel inlet. Here, the fuel drops down onto the bed surface and mixes with bed material. The volatiles are also released here and led into the arms of the volatiles distributor, shown in brown. The volatiles distributor is further discussed in the last paragraph of section 9, Fuel Reactor Design.

8. MORE CONSERVATIVE DESIGN

The design shown above represents an assumed height difference needed to ensure safe transport of material between the reactors. A more conservative approach would be to add, e.g., 0.5 m height for the two loop seals, 0.5 m for the transfer through the FR, 0.3 m for the balconies collecting the wall downflow, and 0.5 m for the inlet to the AR, which raises the height at which the downflow is collected to 7.5 m. Furthermore, the aperture of the two loop seals can be increased simply by lowering the bottom plates of the loop seals, e.g., by 0.5 m, which would increase the horizontal cross section from 2 to 3 m^2 and lower the needed velocity by a third. These changes are seen in Figure 19. Note that these changes do not only increase the driving force for the circulation through the loop seals but also double the pressure difference that can cause leakage between reactors. In the case of ilmenite, this will increase from approximately 6.7 to 13.4 kPa.

It is also possible to increase the width of the loop seals. This can be done by reducing the distance between the loop seals. Presently, there is an effective distance of 1 m between these, that is, an outer distance of 0.2 m plus an insulated wall of 0.4 m. The loop seals can also be further widened if the cross section of the FR is modified from 5 × 4 to 6.6 × 3 m^2, thus lengthening the side parallel to the AR. Consequently, the width of the loop seals could be increased from 2 to 3 m. It would also be possible to double the loop seals leading to the FR and collect downflow at a third wall; thus, the back and front of the boiler would be symmetrical. A top view of such an arrangement is shown in Figure 20. The yellow dashed lines show the channel collecting the downflow along three walls of

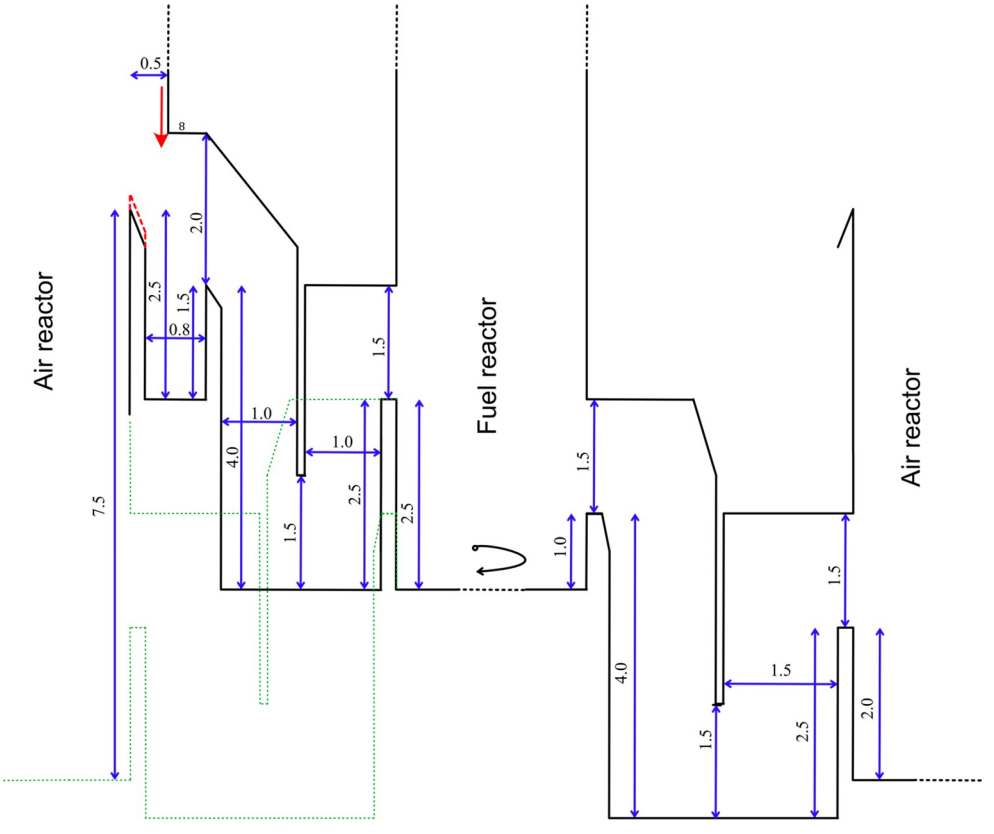

Figure 19. Dimensions of loop seals for a more conservative design.

https://doi.org/10.1021/acs.energyfuels.1c03615
Energy Fuels 2022, 36, 9588−9615

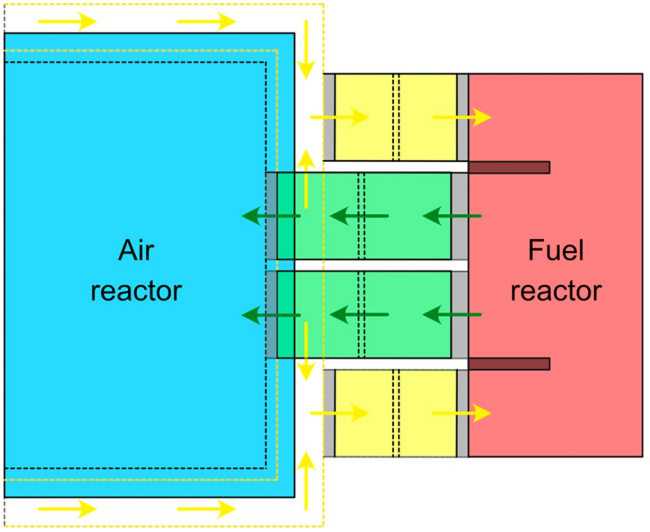

Figure 20. Top view of widened loop seals. The blue area shows the cross section of the AR in the upper part, whereas the black dashed line shows the wall below the collection of downflow along the walls. Yellow dashed lines indicate the channel collecting the downflow. The gray areas show the overflow weirs leading into and out of the loop seals. The double dashed line in the loop seals indicates the underweirs.

the AR. With the increased width and increased height of the aperture, the cross section increases from 2 to 4.5 m^2, which means that the needed horizontal velocity falls from 0.56 to 0.21 m/s, which is within the range suggested by Basu.[143] Table 12 summarizes the design.

9. FUEL REACTOR DESIGN

For the FR, the contact between the oxygen carrier and the combustible gases is a key to reach high performance. Modeling of the results from the solid fuel 100 kW CLC pilot indicates that gas conversion fits with measured kinetics

Table 12. Summary of the Design[a]

	design	conservative design
loop seals		
aperture, height	1	1.5
aperture, width	2	3
aperture, area	2	4.5
aperture flow (t m^{-2} s^{-1})	0.75	0.33
pressure seal height, i.e., top of aperture to outlet	0.5	1
inlet−outlet height	1	1.5
fuel reactor		
inlet height	2	2.5
outlet height	1	1
cross section	5 × 4	6.6 × 3
collection channel		
width	0.8	0.8
height	1.5−2.5	2.5
air reactor		
inlet height	1.5	2
collection height	5.2−5.4	7.5−7.7
lower cross section	4.5 × 7.5	4.5 × 7

[a]Lengths are in meters.

under the assumption that only 15% of the oxygen carrier is in contact with the gas.[144] Studies of operation in a gas-fired 100 kW CLC pilot found the same number, 15%.[145] This is not unexpected, because it is well-known that the major fraction of the gas bypasses the bed in bubbles. Only a small fraction goes through the dense phase. However, a large-scale high-velocity riser provides fundamentally different conditions. Here, particles are elutriated from the bottom bed and proceed upward through the riser, and the contact between gas and elutriated particles is very significantly improved in comparison to the bottom bed.

The pressure drop measurements in three CFB boilers, shown in Figure 13, indicate a significant pressure drop in the riser, e.g., 2−5 kPa above 3 m height, whereas the total pressure drop over the riser is 6−10 kPa. As indicated in, e.g., Figure 13, the pressure drop falls exponentially along the height, because particles leave the upward stream and fall down along the walls. However, with contractions that direct the downflow into the upward stream, the concentration profile can be modified, shifting the pressure drop from the bottom zone to the riser. This has been investigated in a cold-flow model, clearly demonstrating how the pressure drop over the riser can be increased several times through contractions (Figure 21).[146,147] The results were obtained in a cold-flow

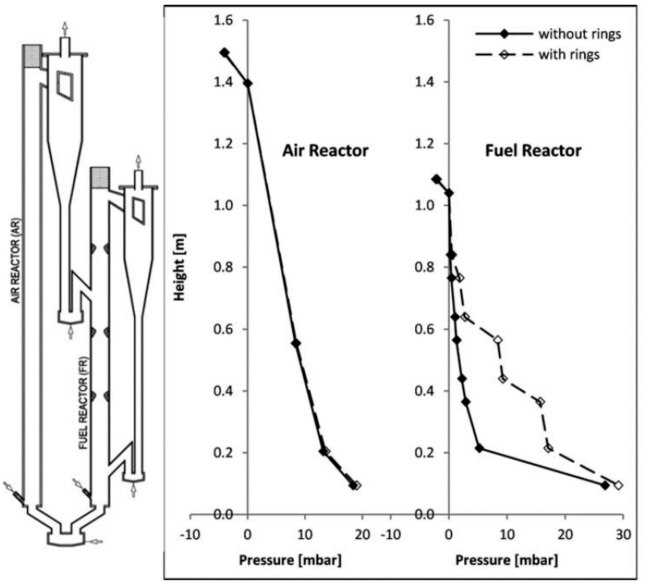

Figure 21. Effect of contractions on the pressure drop over the riser. This figure was reproduced with permission from ref 146. Copyright 2013 John Wiley & Sons.

model simulating a 120 kW CLC reactor system and are not directly applicable to the industrial scale. Nevertheless, there should be little doubt that wedges forcing the downflow along the walls to re-enter the gas stream would improve the gas conversion.

The impact of fluidization conditions is illustrated by the results from pilots of approximately the same fuel power (Table 13). Thus, the Sintef and Chalmers pilots reached similar gas conversion, even though Chalmers had a more reactive oxygen carrier and lower fuel power. A more conspicuous result is the much higher conversion of the pilot in Vienna, where a FR using contractions is used. Here, the amount of unconverted gas is only about a third of the CLC

https://doi.org/10.1021/acs.energyfuels.1c03615
Energy Fuels 2022, 36, 9588−9615

Table 13. Gas Conversion of Woody Biomass in Pilots[a]

pilot	oxygen carrier	fuel power (kW)	gas conversion (%)	carbon capture (%)	diameter (m)	height (m)	temperature (°C)
Chalmers, 100 kW[41,148]	two Mn ores	65−67	65−76	99−100	0.154	5	940−975[149]
TU Vienna, 120 kW[150]	ilmenite	70	up to 93	98	0.128	3	965
Sintef, 150 kW[151]	ilmenite	140	72−77	94−97	0.154	5	960−980
Chalmers, 100 kW[64]	calcium manganate	64	up to 97	99.4−99.5	0.154	5	957

[a]Dimensions and temperatures refer to the FR.

pilots at Chalmers and Sintef. The effect of using a manufactured oxygen carrier with CLOU properties, i.e., calcium manganate, is also included in the last line of Table 13.

Another key aspect of the design of the FR is the fuel feeding. Commonly, fuel is fed above the bottom bed in CFB boilers. This means that the volatiles are mainly released above the bed and close to the fuel feed. In CLC, the fuel should be fed as low as possible in the FR to allow for good contact and high gas conversion. Moving the fuel feed from on top to 10 cm down in the dense bed gave a dramatic improvement of gas conversion in a 10 kW CLC pilot.[39] One option to feed fuel is to feed it into a "box" that is open downward and connected to the bottom of the FR via an underweir.[131] The volatiles will then press the bed level down until they can pass into the FR under the underweir (Figure 22). However, the "box" can be

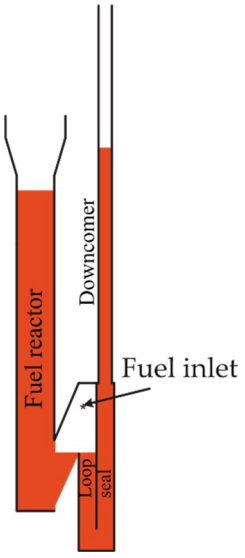

Figure 22. Bottom part of the FR and downcomer of a 100 kW pilot. Fuel is fed into freeboard of the loop seal (LS2) exit side.

elongated to form arms covering the bottom cross section and be given holes on the sides through which the volatiles can pass. Such a volatiles distributor device was proposed by Lyngfelt et al.[152,153,33] and has been further studied in a cold-flow model.[154] The volatiles distributor arms are seen in brown in Figures 16 and 17.

10. AIR REACTOR DESIGN

To accommodate high velocities in the lower section below the balconies, these walls may be uncooled. Furthermore, the bed material collected by the balconies and transferred to the FR needs to have a high temperature, and therefore, cooling of the walls above the balconies must be avoided. To illustrate the need to avoid cooling of the wall layer, measurements in the wall layer of a Chalmers 12 MW CFB indicated that the temperature fell from 850 to around 600 °C, at a distance from the wall, i.e., the fin, of 0.1 and 0.01 m, respectively.[155,156] This does not necessarily mean that these walls need to be uncooled all of the way to the top. As shown by Figures 12 and 13, the concentrations and, consequently, the upward and downward flows fall rapidly with height. Thus, a minor fraction of the downflow reaching the balconies will be collected in the upper part of the riser. If the upper part is cooled, it could nevertheless be a good idea to have wedges between the cooled and uncooled parts to push the particle flow from the walls and into the upward gas stream.

11. DOWNSTREAM TREATMENT

For operation in CLC mode with CO_2 capture, the downstream treatment includes oxygen polishing, particle separation, water condensation, excess oxygen removal, drying, and compression. If the fuel contains nitrogen and sulfur, NO_x and SO_2 removal is also needed.

The downstream system is outlined in Figure 23. The oxygen polishing should be made immediately after the FR.

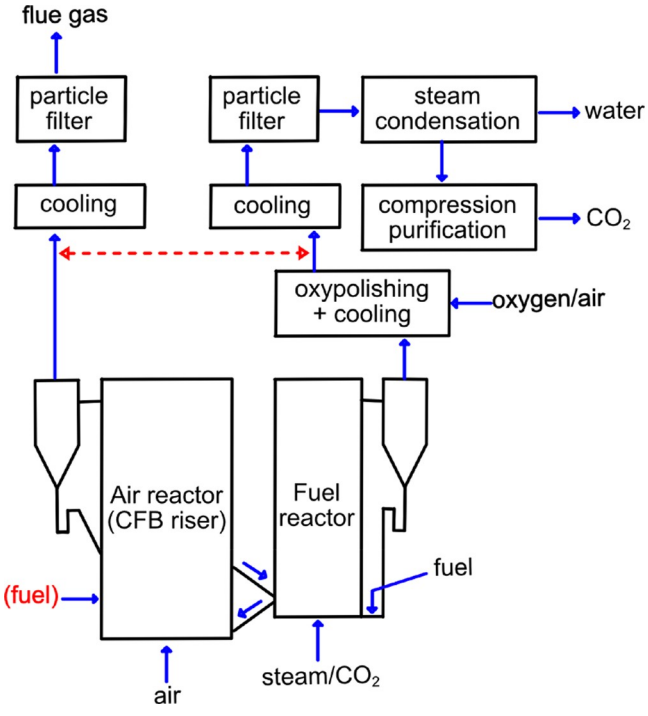

Figure 23. Downstream system.

The downstream treatment will not be discussed in any detail here, but because the gas produced will be similar to that of oxy-fuel combustion, similar process steps can be used for meeting the requirements for CO_2 storage. However, the gas from CLC may have somewhat higher purity than in oxy-fuel, because less oxygen is needed and oxygen to be used in these

https://doi.org/10.1021/acs.energyfuels.1c03615
Energy Fuels 2022, 36, 9588−9615

Table 14. Need for Flexibility for CLC Operation Compared to Normal CFB Combustion

need for flexibility for CLC	impact	countermeasures of the AR
(A) optimal conditions not known	best choice of the temperature, particle size, and oxygen carrier, with gas flows different from expected	changed choice may require any of the countermeasures listed below
(B) lower flows in the AR, because oxygen is consumed without formation of CO_2/H_2O; on the other hand, bottom flow is increased because of no secondary air	although upward solids flow should increase in the bottom part, the flow can be expected to decrease higher up; this would give lower internal circulation via the cyclone; however, it is not clear which effect dominates the circulation to the FR	for internal circulation, no countermeasure is needed; for the case where circulation to the FR needs to increase, see (C)
(C) incomplete gas conversion in the FR	lower air flow to the AR giving lower circulation; less heat produced in the AR/riser giving a lower temperature	circulation: design giving high circulation reduced bed particle size recycling of flue gas increased load, i.e., higher fuel feed to the FR temperature: lowered heat extraction in controllable FBHEs
(D) CLC, the optimal AR/riser temperature expected to be 100−200 °C higher than in combustion	higher AR velocities giving higher circulation; heat extraction needs to be reduced, but higher heat transfer increases heat extration	circulation: increased circulation is an advantage temperature: see (C)
(E) radiative properties changed because radiative gases CO_2 and steam are essentially absent from the AR; additionally, there is no flame radiation	small impact in the AR/riser; small impact in convection pass	superheaters located in FBHEs
(F) partial load	less heat to extract in the AR/riser; lower air flow and, hence, lower circulation; less circulation needed	circulation: see (C) partitioning of AR temperature: see (C)

https://doi.org/10.1021/acs.energyfuels.1c03615
Energy Fuels 2022, 36, 9588−9615

processes is likely not 100% pure. To avoid unnecessary costs for purification, the design should involve solutions that give efficient sealing of the passages downstream of the FR to avoid air ingress.

For a first demonstration of CLC, however, CO_2 capture is not necessary and the costs of the downstream gas treatment, in particular, oxygen production and compression, can be avoided. Thus, air can be used to fully oxidize the gas leaving the FR. After optimal operational conditions and the need for oxygen has been established, necessary steps for producing CO_2 suitable for storage can be added.

12. FLEXIBILITY

There are several reasons why a first large-scale demonstration of CLC boiler needs to be flexible. These will be discussed below.

12.1. Optimal Conditions Are Not Known. It should be possible to use the proposed unit as both a CFB and CLC boiler. There are known differences between these but also uncertainties, e.g., how well CLC will perform with respect to gas conversion. The design and operational strategies need to accommodate these differences and uncertainties. Furthermore, optimal process conditions for CLC in this scale are not known, and it is important that the design allows for exploring the effect of different operational parameters, e.g., the temperature, oxygen carrier, particle size, fuel, and load. Consequently, a first industrial unit should be built to be flexible. Even though this would add costs, these are likely well spent.

12.2. Lower Flows in the Air Reactor. Except for the somewhat narrower bottom part, the CFB riser/AR is dimensioned for 200 MW_{th} when used as a CFB boiler. When used for CLC at the same power, the gas flow in the AR is reduced, and the heat capacity of this flow is even more reduced because the "missing" gases CO_2 and steam have higher heat capacities. On the other hand, the bottom air flow will be increased in the CLC case because no secondary air is used in CLC. This is because there are no gas-phase reactions as in normal combustion. Instead, the air only reacts with the oxygen carrier, i.e., the bed material, and therefore, all of the air should be introduced in the bottom to provide the best contact with the bed material.

12.3. Incomplete Gas Conversion in the Fuel Reactor. In CLC operation, it is expected that the conversion of the gas will not be complete in the FR. If this is not compensated by increased fuel flow to the FR, this means that less heat is produced in the AR and less oxygen is consumed. The corresponding heat would instead be produced by the oxy-polishing step in the post-oxidation chamber. To avoid high air ratios, which increase the energy loss with the flue gas, this will be met with lowered air flow in the AR, but if the flow is reduced too much, this could risk insufficient circulation. One possibility to maintain circulation and velocities is to recycle flue gas, which will not affect the energy loss with the flue gas. This gas can be added above the bottom bed to reduce needed fan power, because the gas will anyway be low in the oxygen concentration. To maintain the temperature in the AR, heat extraction needs to be reduced, using controllable external FBHEs.

Another possibility is that a lower fuel conversion in the FR can be met by increasing the fuel flow to provide adequate reduction of the oxygen carrier and oxygen consumption in the AR. Thus, the heat produced in the AR would remain the same. However, the extra added fuel increases the total thermal power. The extra thermal power is released in the post-oxidation chamber after the FR.

12.4. Higher Optimal Temperature in Chemical Looping Combustion. While a CFB boiler typically operates at 850 °C, the optimal temperature of the AR in CLC may be much higher to provide a high temperature in the FR. Steam gasification of char is greatly enhanced by the increased temperature. Oxygen carrier reactivity with combustibles, in particular, methane, is known to be improved by a higher temperature. Moreover, the temperature in the AR is well below what is needed for thermal NO_x formation; thus, there seems to be no disadvantages of higher temperatures as long as this does not give difficulties with the oxygen carrier. A 100 kW CLC pilot operation with solid fuels has typically used 1025 °C in the AR, for two manganese ores, ilmenite, and calcium manganite,[41,42,64] although temperatures up to 1050 °C have been used. Thus, the optimal temperature for CLC could be 100−200 °C higher. This would raise gas velocity by 9−18%, which at least in part would compensate for the effects of the absence of CO_2 and H_2O and incomplete gas conversion. Further, the heat extraction needs to be reduced, while on the other hand, the heat transfer increases significantly because of the higher temperature. Again, external FBHEs can be used to control the heat extraction.

12.5. Different Radiative Properties of the Gas. With the assumption of no leakage of fuel char into the AR, the gas leaving the reactor will have no CO_2 and very low steam content, e.g., steam present in the combustion air and some steam from the loop seals. Consequently, the radiative capacity of the gas will be low. In addition, there are no flames that contribute with radiation. This should be no major problem in the riser, where elutriated bed material radiates and the wall downflow has an important role in the heat transfer. To meet the need for flexibility and uncooled walls above and below the balconies, more heat exchanger surfaces will be located in FBHEs where radiation has no impact.

12.6. Option for Partial Load. With an increasing share of intermittent renewable energy, the need for part-load operation of boilers will increase. The effect of reducing the load is similar as above, e.g., reduced air flows and circulation and the need for reduced heat extraction to maintain the temperature.

Furthermore, it is also possible to introduce a partitioning wall in the lower part of the AR to divide the chamber into one two sections, with one being closer to the balconies. The latter section could then be fluidized at high velocities, with the other at low velocities. In this way, it would be possible to maintain high circulation with much lower air flow to the AR.

Except for the case where the boiler is used for CO_2 capture, it is not necessary to keep the gases from the FR and AR separated. Thus, part of the gas from the AR can be led to the downstream cooling of the FR as well as in the opposite direction, as illustrated by the dashed red double arrow in Figure 23. This would make the system more flexible with respect to the needed cooling surface in the design. Table 14 summarizes the flexibility needs for the CLC−CFB boiler.

12.7. Fluidization Gas in Loop Seals. Ideally, the fluidization gas for the loop seals connecting the AR and FR should be steam. Nitrogen or air, if going into the FR, would reduce gas purity, whereas CO_2 going into the AR would compromise CO_2 capture. However, when circulation is high, it is expected that the gas flow leaving the loop seal through the inlet side should be low. The circulation flow that drives the

https://doi.org/10.1021/acs.energyfuels.1c03615
Energy Fuels 2022, 36, 9588−9615

mass through the loop seal adds to the particle column on the inlet side and causes bubbles to move toward the outlet side. The upward gas velocity in the dense phase of the column, i.e., the minimum fluidization velocity, would be much lower than the downward flow of solids. Ideally, there would be no bubbles leaking gas to the inlet side. If that would be the case, the loop seal leading to the AR could be fluidized by air and the loop seal leading to the FR could be fluidized by CO_2. More likely is that the pressure fluctuations may lead to some leakage of gases to the inlet side, but the probability of leakage should be lower for fluidization gas injected far from the inlet side.

It could be advisible to divide the fluidization of the loop seal in, e.g., four sections that can be fluidized independently with different gases. Then, it could be investigated whether the sections closest to the outlet can be fluidized by CO_2 or air, without significantly compromising CO_2 gas purity or CO_2 capture.

13. DOWNSTREAM CONVECTION PATHS AND POST-OXIDATION CHAMBER

The convective heat transfer is lowered in CLC by the lower velocity because of the absence of H_2O and CO_2. On the other hand, the heat to be extracted is much lowered because the H_2O and CO_2 gas that exits from the FR contains around 35% of the heat. In part, this is offset by the higher temperature of the gas. In total, the much lower heat to extract should dominate. Consequently, the convection path will have a sufficient heat transfer surface for the CLC case if dimensioned for the CFB boiler case. Incomplete conversion in the FR further reduces gas flow and heat that needs to be extracted.

The convection path after the FR should be able to accommodate increased temperature and flow because of combustion with air/oxygen in the post-oxidation chamber. It is also evident that, if a significant amount of gas burns in the post-oxidation chamber, additional cooling is needed. If the oxygen demand is zero, the heat to be extracted after the FR would be around 40 MW, but the heat extraction would need to increase by approximately 20 MW if the oxygen demand is 10% and by 40 MW if it is 20%. With the assumption that the boiler should have the flexibility to operate under oxygen demands as high as 20%, the flexibility of the convection path should be capable of recovering 40−80 MW of heat. This does not mean that the flexibility would require a 2 times larger heat exchange area. The oxy-polishing will also increase the gas temperature, and the gases consisting of steam and CO_2 have a high radiative emissivity. The radiant heat power is proportional to the fourth power of the absolute temperature, $E = \sigma T^4$, which will raise the heat transfer significantly. The higher gas flow also raises the convective heat transfer. Nevertheless, it is clear that there is a need for the addition of extra heat transfer surfaces in the convection path after the FR to manage the uncertainties with respect to gas conversion.

In normal flame combustion, high temperatures are avoided to minimize thermal NO_x formation. However, the absence or very low concentration of nitrogen in combination with the very low oxygen concentration should make the equilibrium concentration very low, as discussed in the Introduction. Therefore, high temperatures in the post-oxidation chamber are not expected to be a disadvantage.

In CLC operation, less heat is available in the flow from the AR. Thus, for a demonstration where CO_2 is not captured, part of the gases from the FR could be led to the convection pass of the AR, as indicated by the red arrow in Figure 23.

14. USE OF THE FUEL REACTOR IN CFB OPERATION OR GASIFICATION

If, for reasons unknown, the combined CLC−CFB boiler in the end would be used as a CFB boiler, there is the question whether the FR and the associated downstream equipment can be made useful. Because the FR is uncooled, it is obvious that it cannot be used for combustion at any significant load. However, the FR can be used as a combustor if fluidized with a flow of air low enough to avoid high temperatures. Some excess heat could be transferred to the CFB riser. The gases can then be oxidized in the post-oxidation chamber, thus making use of the downstream cooling equipment.

It should also be possible to use the system for combustion with an oxygen carrier and air fluidization of the FR. If the FR is operated with an under-stoichiometric air/fuel ratio, heat generation would move to the AR and final combustion can be accomplished with air in the post-oxidation chamber.

Another option is to use the FR as a thermal gasifier to provide gas, for example, for fuel production. Still another option would be to use it for chemical looping gasification. The advantage with chemical looping gasification compared to normal gasification is that CO_2 will be concentrated to the smaller flue gas exit stream and, therefore, be easier to capture. Thus, if used with biomass, negative emissions can be combined with fuel production.

In conclusion, a dual fluidized bed CLC−CFB boiler could have great flexibility and be operated in different ways for different purposes.

15. OPERATION, STARTUP, AND CONTROL OF CLC

The AR can be started up as a normal CFB boiler, i.e., with startup burners to heat the bed material, after which an increasing flow of solid fuel can be added. Similarly, the FR can be started in parallel, and the FR and all loop seals can be fluidized by air. However, fuel addition to the FR needs to be restricted because the FR is not cooled. As the system reaches the temperature of operation, fluidization of the FR and the loop seals is shifted to steam/CO_2. Then, solid fuel addition is gradually moved from the AR to the FR, keeping careful control of air ratios and temperatures, the latter by use of external fluidized bed heat exchangers. When reduced oxygen carrier particles reach the AR, the oxygen concentration in the outlet gas starts to fall, which is met by reduced fuel addition to the AR. When CLC mode begins, air/oxygen addition to the post-oxidation chamber also needs to start.

The possibility to operate the boiler system as a CFB boiler and gradually shift over to CLC operation in incremental steps should be an important advantage for creating adequate experiences of how to operate the system in chemical looping mode and should also be helpful in achieving high availability of the system.

16. GASEOUS FUELS

Although the boiler design has a focus on solid fuel, it would be an important advantage if the system for fluidizing the FR would be flexible enough to accommodate gaseous fuels, such as natural gas, or, even better, if it would be possible to investigate the use of gases similar to off-gas from SMR. As previously indicated, chemical looping coupled to SMR has a

https://doi.org/10.1021/acs.energyfuels.1c03615
Energy Fuels 2022, 36, 9588−9615

potential for producing blue hydrogen at greatly reduced cost compared to available technologies.

17. COSTS

Although a FR may look big, it does not come with a very large added cost because it is adiabatic, meaning that the walls are not used to produce steam. The walls of the FR, cyclone, downcomer, and post-oxidation chamber would be around 1300 m^2, which, at a cost of 1500 €/m^2,[33] corresponds to 2 M €. With 10 years of appreciation, this would correspond to a yearly cost of 0.2 M€. If 400 000 tonnes of CO_2 are captured every year, this corresponds to an added cost of 0.5 €/tonne of CO_2. As discussed in a previous estimation of costs, the major costs of CLC are compression of CO_2 and production of oxygen for oxygen polishing.[33] Hence, it is possible to significantly reduce the total cost for a first demonstration by starting without CO_2 capture.

18. DISCUSSION

It is commonly assumed that the path of scale-up for the CLC process should proceed via larger pilots before the industrial scale is reached. Thus, at least an intermediate step of the order of 10 MW is foreseen. However, it is evident from the results reported above regarding thermal gasification that dual fluidized bed systems of this size can achieve adequate circulation in sustained operation. Furthermore, the operation with oxygen carrier materials has already been comprehensively tested under various conditions. Although operation in the intermediate size dual fluidized bed system would add additional experience with operation of an oxygen carrier, it will provide little conclusive know-how for the industrial scale. Further, such a demonstration step would take several years from start to delivery of results and could therefore delay the demonstration and commercial implementation of the CLC technology. For energy production, a unit of that size would normally make little sense, which means the investment could be of little value. There is also good reason to question if the costs of building a 10 MW size CLC unit fully equipped for flexible operation would really be less costly than the added costs of building a CFB boiler with a FR and other facilities required for CLC operation, i.e., without CO_2 capture, thus avoiding costs of CO_2 compression and oxygen production in the demonstration stage.

Given the urgent need for carbon-neutral energy production as well as negative CO_2 emissions, there are good reasons for going directly for the industrial-scale demonstration.

19. SUMMARY AND CONCLUSION

Available carbon capture technologies are burdened with high costs and energy penalties for gas separation. CLC provides a way to capture carbon dioxide that avoids gas separation.

There are two key elements for the CLC technology: the first is an oxygen carrier that can transfer oxygen from the combustion air to the fuel through the circulation between the AR and the FR, and the second is sufficient circulation between the two reactors to transfer needed oxygen and heat from the AR to the FR.

Since its first demonstration in 2003, the technology has been well-investigated in a number of smaller pilots with a large number of materials and a total time of operation of around 12 000 h. The work shows that oxygen carrier materials are readily available that meet the requirements of durability, reasonable cost, adequate reactivity, and low risks for health, safety, and environment. Moreover, there is more than 20 000 h of operational experience with oxygen carriers in industrial-scale CFB boilers.

In addition to an adequate oxygen carrier, the process requires sufficient solids circulation. Although adequate circulation has been demonstrated in a large number of smaller pilots, it has not been demonstrated in industrial scale. However, in a similar process, thermal gasification, which requires higher circulation than CLC, sufficient circulation has been well-demonstrated through long-term operation in several plants with a thermal power of 8−32 MW, which would translate to around 3−10 MW if used for CLC.

However, data from large-scale circulating fluidized bed boilers indicate that these are operating under conditions with a circulation much smaller than what is needed in CLC. Reducing the particle size is a way to dramatically increase entrainment of particles in the riser and is a possible way to reach sufficient circulation, although there are uncertainties regarding the impact of increased particle entrainment on the backflow in the riser top. A much higher circulation compared to normal CFB operation would also cause increased losses of bed material from the cyclone and likely require measures to prevent this. Such measures could involve improvement of cyclone performance and the addition of a secondary cyclone.

To avoid these risks and uncertainties, the paper proposes a more robust and simple solution, i.e., to collect the downflow along the riser walls of the AR and lead this to the FR. This downflow, if collected at 5−7 m height, is 1 or 2 orders of magnitude larger than the actual external circulation in a CFB boiler and should be sufficient for the circulation needed in a CLC boiler.

On the basis of this, a design of a combined CLC−CFB boiler has been proposed. The idea is that the boiler can be operated in both CFB and CLC modes or combinations thereof. With a design closely resembling commercial CFB boilers, the technology leap from CFB to CLC can be bridged with a reduced risk. That is, the risk or perceived risk of demonstrating this novel technology would be significantly reduced with the option to use the AR as a CFB boiler. This is because the added costs of the adiabatic FR needed for CLC is reasonably small.

The design is focused on making a highly flexible industrial-scale demonstration boiler, which can be used in CLC operation with different oxygen carriers and different fuels and that can explore different operational strategies to find optimal conditions. The latter involves, e.g., the temperature, load, fluidization gas for the FR, fuel size in the case of solid fuels, solids inventory, oxygen carrier, oxygen carrier size, mixtures of oxygen carriers, and possible additives.

Further, it is recommended that the scaling up of the CLC technology goes directly to industrial-scale demonstration. First, with the great experience already available, it can be questioned whether an intermediate step would really provide any conclusive answers to the key questions that remain to be answered with respect to the industrial-scale operation. Second, an intermediate demonstration would not necessarily be less costly than adding the necessary parts for making an industrial-scale CFB into a CLC−CFB boiler. Moreover, an intermediate size demonstration step would cause unwanted delay of the industrial implementation of CLC.

https://doi.org/10.1021/acs.energyfuels.1c03615
Energy Fuels 2022, 36, 9588−9615

AUTHOR INFORMATION

Corresponding Author

Anders Lyngfelt − *Chalmers University of Technology, 412 96 Göteborg, Sweden;* orcid.org/0000-0002-9561-6574; Email: anders.lyngfelt@chalmers.se

Authors

David Pallarès − *Chalmers University of Technology, 412 96 Göteborg, Sweden;* orcid.org/0000-0002-1574-4075

Carl Linderholm − *Chalmers University of Technology, 412 96 Göteborg, Sweden*

Fredrik Lind − *E.ON Energiinfrastruktur AB, 423 51 Torslanda, Sweden*

Henrik Thunman − *Chalmers University of Technology, 412 96 Göteborg, Sweden*

Bo Leckner − *Chalmers University of Technology, 412 96 Göteborg, Sweden;* orcid.org/0000-0002-4858-7045

Complete contact information is available at: https://pubs.acs.org/10.1021/acs.energyfuels.1c03615

Notes

The authors declare no competing financial interest.

ACKNOWLEDGMENTS

This work was funded by the Swedish National Energy Agency, Project "Chemical-Looping Combustion of Biomass and Waste" (Project 51585-1), and the Swedish Research Council, Project "Biomass Combustion Chemistry with Oxygen Carriers" (Contract 2016-06023).

NOMENCLATURE

AR = air reactor
CCS = carbon capture and storage
CFB = circulating fluidized bed
CLC = chemical looping combustion
CLOU = chemical looping with oxygen uncoupling
EOR = enhanced oil recovery
FBHE = fluidized bed heat exchanger
FR = fuel reactor
MEA = monoethanolamine
OC = oxygen carrier
PSA = pressure swing adsorption
SCR = selective catalytic reduction (of NO)
SMR = steam methane reforming
SNCR = selective non-catalytic reduction (of NO)
WGS = water−gas shift

REFERENCES

(1) Lewis, W.; Gilliland, E.; Sweeney, M. Gasification of carbon. *Chem. Eng. Prog.* **1951**, *47* (5), 251−256.

(2) Lewis, W. K.; Gilliland, E. R. Production of pure carbon dioxide. U.S. Patent 2665972, 1954.

(3) Ishida, M.; Jin, H. A novel combustor based on chemical-looping reactions and its reaction kinetics. *J. Chem. Eng. Jpn.* **1994**, *27* (3), 296−301.

(4) Baylin-Stern, A.; Berghout, N. *Is Carbon Capture Too Expensive?*; https://www.iea.org/commentaries/is-carbon-capture-too-expensive (accessed Feb 17, 2021).

(5) Giannaris, S.; Bruce, C.; Jacobs, B.; Srisang, W.; Janowczyk, D. Implementing a second generation CCS facility on a coal fired powerstation—Results of a feasibility study to retrofit SaskPower's Shand power station with CCS. *Greenhouse Gases Sci. Technol.* **2020**, *10*, 506−518.

(6) IEA Greenhouse Gas R&D Programme (IEAGHG). *Integrated Carbon Capture and Storage Project at Saskpower's Boundary Dam Power Station*; IEAGHG: Cheltenham, U.K., 2015.

(7) Goto, K.; Yogo, K.; Higashii, T. A review of efficiency penalty in a coal-fired power plant withpost-combustion CO_2 capture. *Appl. Energy* **2013**, *111*, 710−720.

(8) Wamsted, D.; Schlissel, D. *Petra Nova Mothballing Post-Mortem: Closure of Texas Carbon Capture Plant Is a Warning Sign*; Institute for Energy Economics and Financial Analysis (IEEFA): Cleveland, OH, 2020; https://ieefa.org/wp-content/uploads/2020/08/Petra-Nova-Mothballing-Post-Mortem_August-2020.pdf (accessed August 3, 2021).

(9) *Boundary Dam Fact Sheet: Carbon Dioxide Capture and Storage Project*; http://sequestration.mit.edu/tools/projects/boundary_dam.html (accessed Sept 30, 2021).

(10) Anonymous. *BD3 Status Update: May 2021*; https://www.saskpower.com/about-us/our-company/blog/2021/bd3-status-update-may-2021 (accessed June 22, 2021).

(11) Schlissel, D. *Boundary Dam 3 Coal Plant Achieves Goal of Capturing 4 Million Metric Tons of CO_2 But Reaches the Goal Two Years Late*; Institute for Energy Economics and Financial Analysis (IEEFA): Cleveland, OH, 2021; http://ieefa.org/wp-content/uploads/2021/04/Boundary-Dam-3-Coal-Plant-Achieves-CO2-Capture-Goal-Two-Years-Late_April-2021.pdf (accessed Dec 9, 2021).

(12) Bruce, C. 92.4% Capture Rate at Petra Nova—That's a CCS Success. *Greenhouse News* **2020**, No. 138, 6−8.

(13) Rao, A. B.; Rubin, E. S.; Berkenpas, M. B. *An Integrated Modeling Framework for Carbon Management Technologies, Volume 1 - Technical Documentation: Amine-Based CO_2 Capture and Storage Systems for Fossil Fuel Power Plant*; National Energy Technology Laboratory (NETL): Pittsburgh, PA, 2004.

(14) *Kemper Project*; https://en.wikipedia.org/wiki/Kemper_Project (accessed Dec 3, 2021).

(15) Nelson, M.; Vimalchand, P.; Brown, R.; Pinkston, T.; Palla, R.; Voelker, D.; Smith, T.; Madden, D. Carbon Capture at the Kemper IGCC Power Plant. *Proceedings of the 14th International Conference on Greenhouse Gas Control Technologies (GHGT-14)*; Melbourne, Victoria, Australia, Oct 21−25, 2018.

(16) Sifat, N. S.; Haseli, Y. A Critical Review of CO_2 Capture Technologies and Prospects for Clean Power Generation. *Energies* **2019**, *12*, 4143.

(17) Komaki, A.; Goto, T.; Uchida, T.; Yamada, T.; Kiga, T.; Spero, C. Operational results of oxyfuel power plant (Callide Oxyfuel Project). *Mech. Eng. J.* **2016**, *3* (6), 16-00342.

(18) Lyngfelt, A.; Kronberger, B.; Adánez, J.; Morin, J.-X.; Hurst, P. The GRACE project. Development of oxygen carrier particles for chemical-looping combustion. Design and operation of a 10 kW chemical-looping combustor. *Proceedings of the 7th International Conference on Greenhouse Gas Control Technologies*; Vancouver, British Columbia, Canada, Sept 5−9, 2004.

(19) Lyngfelt, A.; Thunman, H. Construction and 100 h of operational experience of a 10-kW chemical-looping combustor. *Carbon Dioxide Capture for Storage in Deep Geologic Formations—Results from the CO_2 Capture Project*; Elsevier: Amsterdam, Netherlands, 2005; Vol. *1*, Chapter 36, pp 625−645, DOI: 10.1016/B978-008044570-0/50122-7

(20) Lyngfelt, A.; Johansson, M.; Mattisson, T. Chemical-looping combustion—Status of development. *Proceedings of the 9th International Conference on Circulating Fluidized Beds*; Hamburg, Germany, May 13−16, 2008.

(21) Lyngfelt, A.; Mattisson, T. Materials for chemical-looping combustion. In *Efficient Carbon Capture for Coal Power Plants*; Stolten, D., Scherer, V., Eds.; Wiley-VCH Verlag GmbH & Co. KGaA: Weinheim, Germany, 2011; pp 475−504.

(22) Lyngfelt, A.; Mattisson, T. Oxygen Carriers for Chemical-Looping Combustion. In *Calcium and Chemical Looping Technology for Power Generation and Carbon Dioxide (CO_2) Capture*; Fennell, P., Anthony, E. J., Eds.; Woodhead Publishing: Sawston, U.K., 2014; Chapter 11.

(23) Lyngfelt, A.; Mattisson, T.; Linderholm, C.; Ryden, M. Chemical-Looping Combustion of Solid Fuels—What is Needed to Reach Full-Scale? *Proceedings of the 4th International Conference on Chemical Looping*; Nanjing, China, Sept 26−28, 2016.
(24) Lyngfelt, A.; Linderholm, C. Chemical-Looping Combustion of Solid Fuels—Status and recent progress. *Energy Procedia* **2017**, *114*, 371−386.
(25) Adánez, J.; Abad, A.; Garcia-Labiano, F.; Gayán, P.; de Diego, L. Progress in Chemical-Looping Combustion and Reforming technologies. *Prog. Energy Combust. Sci.* **2012**, *38* (2), 215−282.
(26) Lyngfelt, A.; Brink, A.; Langørgen, Å.; Mattisson, T.; Rydén, M.; Linderholm, C. 11,000 h of Chemical-Looping Combustion Operation—Where Are We and Where Do We Want to Go? *Int. J. Greenhouse Gas Control* **2019**, *88*, 38−56.
(27) Lyngfelt, A. Chemical Looping Combustion: Status and Development Challenges. *Energy Fuels* **2020**, *34*, 9077−9093.
(28) Song, T.; Shen, L. Review of reactor for chemical looping combustion of solid fuels. *Int. J. Greenhouse Gas Control* **2018**, *76*, 92−110.
(29) Abuelgasim, S.; Wang, W.; Abdalazeez, A. A brief review for chemical looping combustion as a promising CO_2 capture technology: Fundamentals and progress. *Sci. Total Environ.* **2021**, *764*, 142892.
(30) Jerndal, E.; Mattisson, T.; Lyngfelt, A. Thermal analysis of chemical-looping combustion. *Chem. Eng. Res. Des.* **2006**, *84* (9), 795−806.
(31) Rydén, M.; Leion, H.; Mattisson, T.; Lyngfelt, A. Combined oxides as oxygen carrier material for chemical-looping with oxygen uncoupling. *Appl. Energy* **2014**, *113*, 1924−1932.
(32) Rydén, M.; Moldenhauer, P.; Lindqvist, S.; Mattisson, T.; Lyngfelt, A. Measuring attrition resistance of oxygen carrier particles for chemical looping combustion with a costumized jet cup. *Powder Technol.* **2014**, *256*, 75−86.
(33) Lyngfelt, A.; Leckner, B. A 1000 MW_{th} Boiler for Chemical-Looping Combustion of Solid Fuels—Discussion of Design and Costs. *Appl. Energy* **2015**, *157*, 475−487.
(34) Linderholm, C.; Schmitz, M. Chemical-Looping Combustion of Solid Fuels in a 100 kW Dual Circulating Fluidized Bed System using Iron Ore as Oxygen Carrier. *J. Environ. Chem. Eng.* **2016**, *4*, 1029−1039.
(35) Pans, M. A.; Gayán, P.; de Diego, L. F.; García-Labiano, F.; Abad, A.; Adánez, J. Performance of a low-cost iron ore as an oxygen carrier for Chemical Looping Combustion of gaseous fuels. *Chem. Eng. Res. Des.* **2015**, *93*, 736−746.
(36) Berguerand, N.; Lyngfelt, A. The use of petroleum coke as fuel in a 10 kW_{th} chemical-looping combustor. *Int. J. Greenhouse Gas Control* **2008**, *2* (2), 169−179.
(37) Linderholm, C.; Knutsson, P.; Schmitz, M.; Markström, P.; Lyngfelt, A. Material balances of carbon, sulfur, nitrogen and ilmenite in a 100 kW CLC reactor system. *Int. J. Greenhouse Gas Control* **2014**, *27*, 188−202.
(38) Moldenhauer, P.; Sundqvist, S.; Mattisson, T.; Linderholm, C. Chemical-Looping Combustion of Synthetic Biomass Volatiles with Manganese-Ore Oxygen Carriers. *Int. J. Greenhouse Gas Control* **2018**, *71*, 239−252.
(39) Linderholm, C.; Lyngfelt, A.; Cuadrat, A.; Jerndal, E. Chemical-looping combustion of solid fuels—Operation in 10 kW unit with two fuels, above-bed and in-bed fuel feed and two oxygen carriers, manganese ore and ilmenite. *Fuel* **2012**, *102*, 808−822.
(40) Schmitz, M.; Linderholm, C.; Hallberg, P.; Sundqvist, S.; Lyngfelt, A. Chemical-Looping Combustion of Solid Fuels using Manganese Ores as Oxygen Carriers. *Energy Fuels* **2016**, *30*, 1204−1216.
(41) Schmitz, M.; Linderholm, C. Chemical looping combustion of biomass in 10 and 100 kW pilots—Analysis of conversion and lifetime using a sintered manganese ore. *Fuel* **2018**, *231*, 73−84.
(42) Linderholm, C.; Schmitz, M.; Biermann, M.; Hanning, M.; Lyngfelt, A. Chemical-looping combustion of solid fuel in a 100 kW unit using sintered manganese ore as oxygen carrier. *Int. J. Greenhouse Gas Control* **2017**, *65*, 170−181.
(43) Moldenhauer, P.; Linderholm, C.; Rydén, M.; Lyngfelt, A. Avoiding CO_2 capture effort and cost for negative CO_2 emissions using industrial waste in chemical-looping combustion/gasification of biomass. *Mitigation Adapt. Strategies Global Change* **2020**, *25*, 1−24.
(44) Källén, M.; Rydén, M.; Dueso, C.; Mattisson, T.; Lyngfelt, A. $CaMn_{0.9}Mg_{0.1}O_{3-\delta}$ as Oxygen Carrier in a Gas-Fired 10 kW_{th} Chemical-Looping Combustion Unit. *Ind. Eng. Chem. Res.* **2013**, *52*, 6923−6932.
(45) Cabello, A.; Abad, A.; Gayán, P.; García-Labiano, F.; de Diego, L. F.; Adánez, J. Increasing energy efficiency in chemical looping combustion of methane by in-situ activation of perovskite-based oxygen carriers. *Appl. Energy* **2021**, *287*, 116557.
(46) Hallberg, P.; Hanning, M.; Rydén, M.; Mattisson, T.; Lyngfelt, A. Investigation of a calcium manganite as oxygen carrier during 99 h of operation of Chemical-Looping Combustion in a 10 kW-unit. *Int. J. Greenhouse Gas Control* **2016**, *53*, 222−229.
(47) Moldenhauer, P.; Hallberg, P.; Biermann, M.; Snijkers, F.; Albertsen, K.; Mattisson, T.; Lyngfelt, A. Oxygen-Carrier Development of Calcium Manganite-Based Materials with Perovskite Structure for Chemical-Looping Combustion of Methane. *Energy Technol.* **2020**, *8*, 2000069.
(48) Ohlemüller, P.; Reitz, M.; Ströhle, J.; Epple, B. Investigation of chemical looping combustion of natural gas at 1 MW_{th} scale. *Proc. Combust. Inst.* **2019**, *37* (4), 4353−4360.
(49) Gayán, P.; Forero, C. R.; Abad, A.; De Diego, L. F.; García-Labiano, F.; Adánez, J. Effect of support on the behavior of Cu-based oxygen carriers during long-term CLC operation at temperatures above 1073 K. *Energy Fuels* **2011**, *25* (3), 1316−1326.
(50) Adánez-Rubio, I. A.; Bararpour, S. T.; Abad, A.; Gayán, P.; Williams, G.; Scullard, A.; Mahinpey, N.; Adánez, J. Performance Evaluation of a Cu-Based Oxygen Carrier Impregnated onto ZrO_2 for Chemical-Looping Combustion (CLC). *Ind. Eng. Chem. Res.* **2020**, *59*, 7255−7266.
(51) Schmitz, M.; Linderholm, C.; Lyngfelt, A. Chemical-Looping Combustion of Four Different Solid Fuels using a Manganese-Silicon-Titanium Oxygen Carrier. *J. Greenhouse Gas Control* **2018**, *70*, 88−96.
(52) Linderholm, C.; Mattisson, T.; Lyngfelt, A. Long-term integrity testing of spray-dried particles in a 10-kW chemical-looping combustor using natural gas as fuel. *Fuel* **2009**, *88*, 2083−2096.
(53) Corcoran, A.; Knutsson, P.; Thunman, H.; Lind, F. Industrial Implementation of Oxygen Carrier Aided Combustion. *Proceedings of the 5th International Conference on Chemical Looping*; Park City, UT, Sept 24−27, 2018.
(54) Lind, F.; Corcoran, A.; Andersson, B.-Å.; Thunman, H. 12,000 h of operation with oxygen-carriers in industrially relevant scale. *VGB PowerTech J.* **2017**, *7*, 82−87.
(55) Andersson, B.-Å.; Lind, F.; Corcoran, A.; Thunman, H. 4000 h of Operation with Oxygen-Carriers in Industrial Relevant Scale (75 MW_{th}). *Proceedings of the 4th International Conference on Chemical Looping*; Nanjing, China, Sept 26−28, 2016.
(56) Moldenhauer, P.; Corcoran, A.; Thunman, H.; Lind, F. A Scale-Up Project for Operating a 115 MW_{th} Biomass-Fired CFB Boiler with Oxygen Carriers as Bed Material. *Proceedings of the 5th International Conference on Chemical Looping*; Park City, UT, Sept 24−27, 2018.
(57) Vilches, T. B.; Lind, F.; Rydén, M.; Thunman, H. Experience of more than 1000 h of operation with oxygen carriers and solid biomass at large scale. *Appl. Energy* **2017**, *190*, 1174−1183.
(58) Gyllén, A.; Knutsson, P.; Lind, F.; Thunman, H. Magnetic separation of ilmenite used as oxygen carrier during combustion of biomass and the effect of ash layer buildup on its activity and mechanical strength. *Fuel* **2020**, *269*, 117470.
(59) Rydén, M.; Hanning, M.; Corcoran, A.; Lind, F. Oxygen carrier aided combustion (OCAC) of wood chips in a semi-commercial circulating fluidized bed boiler using manganese ore as bed material. *Appl. Sci.* **2016**, *6*, 347.
(60) Adánez, J.; Abad, A.; Mendiara, T.; Gayán, P.; de Diego, L. F.; García-Labiano, F. Chemical looping combustion of solid fuels. *Prog. Energy Combust. Sci.* **2018**, *65*, 6−66.

https://doi.org/10.1021/acs.energyfuels.1c03615
Energy Fuels 2022, 36, 9588−9615

(61) Lyngfelt, A. Oxygen carriers for chemical-looping combustion—4000 h of operational experience. *Oil Gas Sci. Technol.* **2011**, *66* (2), 161−172.
(62) Berguerand, N.; Lyngfelt, A. Design and operation of a 10 kWth chemical-looping combustor for solid fuels—Testing with South African coal. *Fuel* **2008**, *87* (12), 2713−2726.
(63) Pikkarainen, T.; Hiltunen, I.; Teir, S. Piloting of bio-CLC for BECCS. *Proceedings of the 4th International Conference on Chemical Looping*; Nanjing, China, Sept 26−28, 2016.
(64) Gogolev, I.; Linderholm, C.; Gall, D.; Schmitz, M.; Mattisson, T.; Pettersson, J. B. C.; Lyngfelt, A. Chemical-Looping Combustion in a 100 kW Unit Using a Mixture of Synthetic and Natural Oxygen Carriers—Operational Results and Fate of Biomass Fuel Alkali. *Int. J. Greenhouse Gas Control* **2019**, *88*, 371−382.
(65) Normann, F.; Wismer, A.; Müller, C.; Leion, H. Oxidation of ammonia by iron, manganese and nickel oxides—Implications on NO_x formation in chemical-looping combustion. *Fuel* **2019**, *240*, 57−63.
(66) Markström, P.; Linderholm, C.; Lyngfelt, A. Chemical-looping combustion of solid fuels—Design and operation of a 100 kW unit with bituminous coal. *Int. J. Greenhouse Gas Control* **2013**, *15*, 150−162.
(67) Pérez-Astray, A.; Adánez-Rubio, I.; Mendiara, T.; Izquierdo, M. T.; Abad, A.; Gayán, P.; de Diego, L. F.; García-Labiano, F.; Adánez, J. Comparative study of fuel-N and tar evolution in chemical loopingcombustion of biomass under bothiG-CLC and CLOU modes. *Fuel* **2019**, *236*, 598−607.
(68) Ajdari, S.; Garðarsdòttir, S.; Normann, F.; Andersson, K. *Techno-economic Evaluation of Integrated NO_x and SO_x Removal in Pressurized Flue Gas Systems for Carbon Capture Applications*; Chalmers University of Technology: Göteborg, Sweden, 2019; http://www.entek.chalmers.se/lyngfelt/co2/357Ajdari_NOxSOxRemoval_PaperIV.pdf.
(69) Ekström, C.; Schwendig, F.; Biede, O.; Franco, F.; Haupt, G.; de Koeijer, G.; Papapavlou, C.; Røkke, P. E. Techno-Economic Evaluations and Benchmarking of Pre-combustion CO_2 Capture and Oxy-fuel Processes Developed in the European ENCAP Project. *Energy Procedia* **2009**, *1*, 4233−4240.
(70) Anonymous. The costs of CO_2 capture—Post-demonstration CCS in the EU—Zero Emission Platform; *European Technology Platform for Zero Emission Fossil Fuel Power Plants (ZEP)*; European Technology and Innovation Platform (ETIP) Bioenergy: Brussels, Belgium, 2011.
(71) Ohlemüller, P.; Olausson, M.; John, M.; Alobaid, F.; Ströhle, J.; Epple, B. Thermodynamic and Economic Evaluation of a Full Scale Chemical Looping Plant. *Proceedings of the 5th International Conference on Chemical Looping*; Park City, UT, Sept 24−27, 2018.
(72) Haaf, M.; Ohlemüller, P.; Ströhle, J.; Epple, B. Assessment of the Potential for Negative CO_2 Emissions by the Utilization of Alternative Fuels in 2nd Generation CCS Processes. *Proceedings of the International Conference on Negative CO_2 Emissions*; Göteborg, Sweden, May 22−24, 2018.
(73) Mattisson, T.; Lyngfelt, A.; Leion, H. Chemical-looping with oxygen uncoupling for combustion of solid fuels. *Int. J. Greenhouse Gas Control* **2009**, *3* (1), 11−19.
(74) Lyngfelt, A.; Mattisson, T. Trestegsförbränning för avskiljning av koldioxid (Chemical-looping with oxygen uncoupling for separation of carbon dioxide). Swedish Patent Application 05002498, 2005.
(75) Mattisson, T.; Leion, H.; Lyngfelt, A. Chemical-looping with oxygen uncoupling using CuO/ZrO_2 with petroleum coke. *Fuel* **2009**, *88* (4), 683−690.
(76) Lyngfelt, A.; Mattisson, T.; Shulman, A.; Cleverstam, E. Nya syrebärare för två- och/eller trestegsförbränning (New oxygen carriers for chemical-looping combustion and/or chemical-looping combustion with oxygen uncoupling). Swedish Patent 534428 C2, 2009.
(77) Shulman, A.; Cleverstam, E.; Mattisson, T.; Lyngfelt, A. Manganese/Iron, Manganese/Nickel, and Manganese/Silicon oxides Used in Chemical-Looping with Oxygen Uncoupling (CLOU) for combustion with methane. *Energy Fuels* **2009**, *23*, 5269−5275.
(78) Shulman, A.; Cleverstam, E.; Mattisson, T.; Lyngfelt, A. Chemical-Looping with Oxygen Uncoupling using Mn/Mg-based Oxygen Carriers for Methane Combustion. *Fuel* **2011**, *90*, 941−950.
(79) Azimi, G.; Leion, H.; Mattisson, T.; Lyngfelt, A. Chemical-looping with oxygen uncoupling using combined Mn-Fe oxides, testing in batch fluidized bed. *Energy Procedia* **2011**, *4*, 370−377.
(80) Azimi, G.; Rydén, M.; Leion, H.; Mattisson, T.; Lyngfelt, A. $(Mn_yFe_{1-y})O_x$ combined oxides as oxygen carrier for chemical-looping combustion with oxygen uncoupling (CLOU). *AIChE J.* **2013**, *59* (2), 582−588.
(81) Hanning, M.; Frick, V.; Mattisson, T.; Rydén, M.; Lyngfelt, A. The Performance of Combined Manganese-Silicon Oxygen Carriers and the Possible Effects of Adding Titania. *Energy Fuels* **2016**, *30*, 1171−1182.
(82) Källén, M.; Hallberg, P.; Rydén, M.; Mattisson, T.; Lyngfelt, A. Combined Oxides of Iron, Manganese and Silica as Oxygen Carriers for Chemical-Looping with Oxygen Uncoupling. *Fuel Process. Technol.* **2014**, *124*, 87−96.
(83) Källén, M.; Rydén, M.; Lyngfelt, A.; Mattisson, T. Chemical-looping combustion using combined iron/manganese/silicon oxygen carriers. *Appl. Energy* **2015**, *157*, 330−337.
(84) Rydén, M.; Lyngfelt, A.; Mattisson, T. Combined manganese/iron oxides as oxygen carrier for chemical looping combustion with oxygen uncoupling (CLOU) in a circulating fluidized bed reactor system. *Energy Procedia* **2011**, *4*, 341−348.
(85) Mattisson, T.; Jing, D.; Lyngfelt, A.; Rydén, M. Experimental investigation of binary and ternary combined manganese oxides for chemical-looping with oxygen uncoupling (CLOU). *Fuel* **2016**, *164*, 228−236.
(86) Moldenhauer, P.; Hallberg, P.; Biermann, M.; Snijkers, F.; Albertsen, K.; Mattisson, T.; Lyngfelt, A. Oxygen carrier development of calcium manganite-based materials with perovskite structure for chemical looping combustion of methane. *Proceedings of the 42nd International Technical Conference on Clean Energy*; Clearwater, FL, June 11−15, 2017.
(87) Rydén, M.; Lyngfelt, A.; Mattisson, T. $CaMn_{0.875}Ti_{0.125}O_3$ as oxygen carrier for chemical-looping combustion with oxygen uncoupling (CLOU)—Experiments in continuously operating fluidized bed reactor system. *Int. Journal of Greenhouse Gas Control* **2011**, *5*, 356−366.
(88) Hallberg, P.; Källén, M.; Jing, D.; Snijkers, F.; van Noyen, J.; Rydén, M.; Lyngfelt, A. Experimental investigation of $CaMnO_{3-\delta}$ based oxygen carriers used in continuous chemical-looping combustion. *Int. J. Chem. Eng.* **2014**, *2014*, 412517.
(89) Hallberg, P.; Rydén, M.; Mattisson, T.; Lyngfelt, A. $CaMnO_{3-\delta}$ made from low cost material examined as oxygen carrier in Chemical-Looping Combustion. *Energy Procedia* **2014**, *63*, 80−86.
(90) Schmitz, M.; Linderholm, C.; Lyngfelt, A. Chemical Looping Combustion of Sulfurous Solid Fuels using Calcium Manganite as Oxygen Carrier. *Energy Procedia* **2014**, *63*, 140−152.
(91) Schmitz, M.; Linderholm, C. Performance of calcium Manganite as oxygen carrier in chemical looping combustion of biomass in a 10 kW pilot. *Appl. Energy* **2016**, *169*, 729−737.
(92) Cabello, A.; Abad, A.; Gayán, P.; de Diego, L. F.; García-Labiano, F.; Adánez, J. Effect of operating conditions and H_2S presence on the performance of $CaMg_{0.1}Mn_{0.9}O_{3-\delta}$ perovskite material in chemical looping combustion (CLC). *Energy Fuels* **2014**, *28* (2), 1262−1274.
(93) Mattisson, T.; Adánez, J.; Mayer, K.; Snijkers, F.; Williams, G.; Wesker, E.; Bertsch, O.; Lyngfelt, A. Innovative Oxygen Carriers Uplifting Chemical-looping Combustion. *Energy Procedia* **2014**, *63*, 113−130.
(94) Mayer, K.; Penthor, S.; Pröll, T.; Hofbauer, H. The different demands of oxygen carriers on the reactor system of a CLC plant—Results of oxygen carrier testing in a 120 kW_{th} pilot plant. *Appl. Energy* **2015**, *157*, 323−329.

https://doi.org/10.1021/acs.energyfuels.1c03615
Energy Fuels 2022, 36, 9588−9615

(95) Ohlemüller, P.; Reitz, M.; Ströhle, J.; Epple, B. Operation of a 1 MW_{th} chemical looping pilot plant with natural gas. *Proceedings of the High Temperature Solid Looping Cycles Network*; Luleå, Sweden, Sept 4−5, 2017.
(96) Ohlemüller, P.; Reitz, M.; Ströhle, J.; Epple, B. Operation of a 1 MW_{th} chemical looping pilot plant with natural gas. *Proceedings of the 9th Trondheim Conference on CO_2 Capture, Transport and Storage*; Trondheim, Norway, June 12−14, 2017.
(97) Tilland, A.; Lambert, A.; Pelletant, W.; Chiche, D.; Bounie, C.; Bertholin, S. Comparison of two oxygen carriers performances for chemical looping combustion application. *Proceedings of the 9th Trondheim Conference on CO_2 Capture, Transport and Storage*; Trondheim, Norway, June 12−14, 2017.
(98) Moldenhauer, P.; Rydén, M.; Mattisson, T.; Jamal, A.; Lyngfelt, A. Chemical-Looping Combustion with Heavy Liquid Fuels in a 10 kW Pilot Plant. *Fuel Process. Technol.* **2017**, *156*, 124−137.
(99) Penthor, S.; Mattisson, T.; Adánez, J.; Bertolin, S.; Masi, E.; Larring, Y.; Langørgen, Å.; Ströhle, J.; Snijkers, F.; Geerts, L.; Albertsen, K.; Williams, G.; Bertsch, O.; Authier, O.; Dávila, Y.; Yazdanpanah, M.; Pröll, T.; Lyngfelt, A.; Hofbauer, H. The EU-FP7 project SUCCESS—Scale-up of oxygen carrier for chemical looping combustion using environmentally sustainable materials. *Energy Procedia* **2017**, *114*, 395−406.
(100) Jackson, S.; Brodal, E. Optimization of the Energy Consumption of a Carbon Capture and Sequestration Related Carbon Dioxide Compression Processes. *Energies* **2019**, *12*, 1603.
(101) Quang, D. V.; Rabindran, A. V.; Hadri, N. E.; Abu-Zahra, M. R. M. Reduction in the Regeneration Energy of CO_2 Capture Process by Impregnating Amine Solvent onto Precipitated Silica. *Eur. Sci. J.* **2013**, *9* (30), 82−102.
(102) Tatsumi, M.; Yagi, Y.; Kadono, K.; Kaibara, K.; Iijima, M.; Ohishi, T.; Tanaka, H.; Hirata, T.; Mitchell, R. New Energy Efficient Processes and Improvements for Flue Gas CO_2 Capture. *Energy Procedia* **2011**, *4*, 1347−1352.
(103) Xiong, J.; Zhao, H.; Zheng, C. Thermoeconomic cost analysis of a 600 MW_e oxy-combustion pulverized-coal-fired power plant. *Int. J. Greenhouse Gas Control* **2012**, *9*, 469−483.
(104) Janusz-Szymańska, K.; Dryjańska, A. Possibilities for improving the thermodynamic and economic characteristics of an oxy-type power plant with a cryogenic air separation unit. *Energy* **2015**, *85*, 45−61.
(105) Anonymous.. Technologies for Direct Air Capture of CO^2. *Carbon Capture J.* **2021**, 13−14.
(106) Corcoran, A.; Knutsson, P.; Lind, F.; Thunman, H. Mechanism for Migration and Layer Growth of Biomass Ash on Ilmenite Used for Oxygen Carrier Aided Combustion. *Energy Fuels* **2018**, *32*, 8845−8856.
(107) Hanning, M.; Corcoran, A.; Lind, F.; Rydén, M. Biomass ash interactions with a manganese ore used as oxygen-carrying bed material in a 12 MW_{th} CFB boiler. *Biomass Bioenergy* **2018**, *119*, 179−190.
(108) Gogolev, I.; Soleimanisalim, A.; Linderholm, C.; Lyngfelt, A. Commissioning, Performance Benchmarking, and Investigation of Alkali Emissions in a 10 kW_{th} Solid Fuel Chemical Looping Combustion Pilot. *Fuel* **2021**, *287*, 119530.
(109) Gogolev, I.; Pikkarainen, T.; Kauppinen, J.; Linderholm, C.; Steenari, B.-M.; Lyngfelt, A. Investigation of Biomass Alkali Release in a Dual Circulating Fluidized Bed Chemical Looping Combustion System. *Fuel* **2021**, *297*, 120743.
(110) Stenberg, V.; Spallina, V.; Mattisson, T.; Rydén, M. Techno-economic analysis of H_2 production processes using fluidized bed heat exchangers with steam reforming—Part 2: Chemical-looping combustion. *Int. J. Hydrogen Energy* **2021**, *46*, 25355−25375.
(111) Lyngfelt, A. SMR-CLC = the perfect match for blue hydrogen? *Carbon Capture J.* **2021**, 24−25.
(112) Hallberg, P.; Leion, H.; Lyngfelt, A. A method for determination of reaction enthalpy of oxygen carriers for Chemical Looping Combustion—Application to ilmenite. *Thermochim. Acta* **2011**, *524*, 62−67.
(113) Proll, T.; Rauch, R.; Aichernig, C.; Hofbauer, H. Fluidized Bed Steam Gasification of Solid Biomass—Performance Characteristics of an 8 MW_{th} Combined Heat and Power Plant. *Int. J. Chem. React. Eng.* **2007**, *5*, 937−944.
(114) Larsson, A.; Kuba, M.; Berdugo Vilches, T.; Seemann, M.; Hofbauer, H.; Thunman, H. Steam gasification of biomass—Typical gas quality and operational strategies derived from industrial-scale plants. *Fuel Process. Technol.* **2021**, *212*, 106609.
(115) Leckner, B. Fluid dynamic regimes in circulating fluidized bed boilers—A mini-review. *Chem. Eng. Sci.* **2022**, *247*, 117089.
(116) Johnsson, F.; Leckner, B. Vertical distribution of solids in a CFB-furnace. *Proceedings of the 13th International Conference on Fluidized Bed Technology*; Orlando, FL, May 7−10, 1995; pp 671−679.
(117) Djerf, T. Solids Flow in Large-Scale Circulating Fluidized Bed Furnaces. Ph.D. Thesis, Chalmers University of Technology, Göteborg, Sweden, 2021.
(118) Linderholm, C.; Schmitz, M.; Knutsson, P.; Lyngfelt, A. Chemical-Looping Combustion in a 100-kW Unit using a Mixture of Ilmenite and Manganese Ore as Oxygen Carrier. *Fuel* **2016**, *166*, 533−542.
(119) Yue, G.; Lu, J.; Zhang, H.; Yang, H.; Zhang, J.; Liu, Q.; Li, Z.; Joos, E.; Jaud, P. Design theory of circulating fluized bed boilers. *Proceedings of the 18th International Conference on Fluidized Bed Combustion*; Toronto, Ontario, Canada, May 22−25, 2005.
(120) Wu, H.; Zhang, M.; Sun, Y.; Lu, Q.; Na, Y. Research on the heat transfer model of platen heating surface of 300 MW circulating fluidized bed boilers. *Powder Technol.* **2012**, *226*, 83−90.
(121) Redemann, K.; Hartge, E.-U.; Werther, J. A particle population balancing model for a circulating fluidized bed combustion system. *Powder Technol.* **2009**, *191*, 78−90.
(122) Blaszczuk, A.; Leszczynski, J.; Nowak, W. Simulation model of the mass balance in a supercritical circulating fluidized bed combustor. *Powder Technol.* **2013**, *246*, 317−326.
(123) Blaszczuk, A.; Nowak, W.; Krzywanski, J. Effect of Bed Particle Size on Heat Transfer between Fluidized Bed of Group B Particles and Vertical Rifled Tubes. *Powder Technol.* **2017**, *316*, 111−122.
(124) Li, D.; Cai, R.; Zhang, M.; Yang, H.; Choi, K.; Ahn, S.; Jeon, C.-H. Operation characteristics of a bubbling fluidized bed heat exchanger with internal solid circulation for a 550-MW_e ultra-supercritical CFB boiler. *Energy* **2020**, *192*, 116503.
(125) Li, D.; Ke, X.; Zhang, M.; Yang, H.; Jung, S.; Ahn, S.; Jeon, C.-H. A comprehensive mass balance model of a 550 MW_e ultra-supercritical CFB boiler with internal circulation. *Energy* **2020**, *206*, 117941.
(126) Edvardsson, E.; Åmand, L.-E.; Thunman, H.; Leckner, B.; Johnsson, F. Measuring the External Solids Flux in a CFB boiler. *Proceedings of the 19th Fluidized Bed Combustion (FBC) Conference*; Vienna, Austria, May 21−24, 2006.
(127) Johnsson, F.; Zhang, W.; Leckner, B. Characteristics of the formation of particle wall layers in CFB boilers. *Proceedings of the Second International Conference on Multiphase Flow*; Kyoto, Japan, April 3−7, 1995; pp 25−32.
(128) Johnsson, F.; Vrager, A.; Leckner, B. Solids flow pattern in the exit region of a CFB-furnace—Influence of exit geometry. *Proceedings of the 15th International Conference on Fluidized Bed Combustion*; Savannah, GA, May 16−19, 1999.
(129) Johansson, A.; Johnsson, F.; Leckner, B. Solids back-mixing in CFB boilers. *Chem. Eng. Sci.* **2007**, *62*, 561−573.
(130) Djerf, T.; Pallarès, D.; Johnsson, F. Solids flow patterns in large-scale circulating fluidised bed boilers: Experimental evaluation under fluid-dynamically down-scaled conditions. *Chem. Eng. Sci.* **2021**, *231*, 116309.
(131) Markström, P.; Lyngfelt, A. Designing and operating a cold-flow model of a 100 kW chemical-looping combustor. *Powder Technol.* **2012**, *222*, 182−192.
(132) Linderholm, C.; Schmitz, M.; Lyngfelt, A. Estimating the solids circulation rate in a 100-kW chemical looping combustor. *Chem. Eng. Sci.* **2017**, *171*, 351−359.

https://doi.org/10.1021/acs.energyfuels.1c03615
Energy Fuels 2022, 36, 9588−9615

(133) Lyngfelt, A.; Leckner, B.; Mattisson, T. A fluidized-bed combustion process with inherent CO_2 separation; Application of chemical-looping combustion. *Chem. Eng. Sci.* **2001**, *56* (10), 3101−3113.
(134) Marx, K.; Pröll, T.; Hofbauer, H. Next Scale Chemical-Looping Combustion: Fluidized Bed System Design for Demonstration Unit. *Proceedings of the 21st International Conference on Fluidized Bed Combustion*; Naples, Italy, June 3−6, 2012; Vol. *1*, pp 269−276.
(135) Bi, H.; Grace, J. R. Flow Regime Diagrams for Gas-Solid Fluidization and Upward Transport. *Int. J. Multiphase Flow* **1995**, *21* (6), 1229−1236.
(136) Abad, A.; Adánez, J.; Gayán, P.; de Diego, L. F.; García-Labiano, F.; Sprachmann, G. Conceptual design of a 100 MW_{th} CLC unit for solid fuel combustion. *Appl. Energy* **2015**, *157*, 462−474.
(137) Sharma, R.; Chandel, M. K.; Delebarre, A.; Alappat, B. 200-MW chemical looping combustion based thermal power plant for clean power generation. *Int. J. Energy Res.* **2013**, *37*, 49−58.
(138) Pallarès, D.; Johnsson, F. Macroscopic modelling of fluid dynamics in large-scale circulating fluidized beds. *Prog. Energy Combust. Sci.* **2006**, *32* (5−6), 539−569.
(139) Werdermann, C. C. Feststoffbewegung und Wärmeübergang in zirkulierenden Wirbelschichten von Kohlekraftwerken. Ph.D. Thesis, Hamburg University of Technology, Hamburg, Germany, 1993.
(140) Suraniti, S.; Guilleux, E.; Morin, J. X. Utility CFB furnace wall hydrodynamics. *Proceedings of the International Conference on Circulating Fluidized Beds (CFB-6)*; Würzburg, Germany, Aug 22−27, 1999.
(141) Ströhle, J.; Orth, M.; Epple, B. Chemical Looping Combustion of Hard Coal in a 1 MW_{th} Pilot Plant Using Ilmenite as Oxygen Carrier. *Appl. Energy* **2015**, *157*, 288−294.
(142) Ohlemüller, P.; Busch, J.-P.; Reitz, M.; Ströhle, J.; Epple, B. Chemical-Looping Combustion of Hard Coal: Autothermal Operation of a 1 MW_{th} Pilot Plant. *J. Energy Resour. Technol.* **2016**, *138* (4), 042203.
(143) Basu, P. *Circulating Fluidized Bed Boilers—Design, Operation and Maintenance*; Springer: Heidelberg, Germany, 2015.
(144) Markström, P.; Linderholm, C.; Lyngfelt, A. Analytical model of gas conversion in a 100 kW chemical-looping combustor for solid fuels—Comparison with operational results. *Chem. Eng. Sci.* **2013**, *96*, 131−141.
(145) Kolbitsch, P.; Pröll, T.; Hofbauer, H. Modeling of a 120 kW chemical looping combustion reactor system using a Ni-based oxygen carrier. *Chem. Eng. Sci.* **2009**, *64* (1), 99−108.
(146) Guío-Pérez, D. C.; Hofbauer, H.; Pröll, T. Effect of Ring-Type Internals on Solids Distribution in a Dual Circulating Fluidized Bed System—Cold Flow Model Study. *AIChE J.* **2013**, *59* (10), 3612−3623.
(147) Guío-Pérez, D. C.; Pröll, T.; Hofbauer, H. Influence of ring-type internals on the solids residence time distribution in the fuel reactor of adual circulating fluidized bed system for chemical looping combustion. *Chem. Eng. Res. Des.* **2014**, *92*, 1107−1118.
(148) Schmitz, M.; Linderholm, C.; Lyngfelt, A. Operational Experience of CO_2 Capture Using Chemical-Looping Combustion of Biomass-based Fuels in a 100 kW Unit. *Proceedings of the International Conference on Negative CO_2 Emissions*; Göteborg, Sweden, May 22−24, 2018.
(149) Linderholm, C.; Lyngfelt, A.; Rydén, M.; Schmitz, M. Chemical-looping combustion of biomass in a 100 kW pilot. *Proceedings of the European Biomass Conference and Exhibition (EUBCE) 2017*; Stockholm, Sweden, June 12−15, 2017; pp 412−415.
(150) Penthor, S.; Fuchs, J.; Benedikt, F.; Schmid, J. C.; Mauerhofer, A. M.; Mayer, K.; Hofbauer, H. First results from an 80 kW dual fluidized bed pilot unit for solid fuels at TU Wien. *Proceedings of the 5th International Conference on Chemical Looping*; Park City, UT, Sept 24−27, 2018.
(151) Langørgen, Å.; Saanum, I. Chemical looping combustion of wood pellets in a 150 kW_{th} CLC reactor. *Proceedings of the International Conference on Negative CO_2 Emissions*; Göteborg, Sweden, May 22−24, 2018.
(152) Lyngfelt, A.; Pallarés, D.; Linderholm, C.; Rydén, M.; Mattisson, T. "Fördelare av gaser i fluidiserad bädd" ("Distributor of volatile gases in the bottom part of a fluidized bed"). Swedish Patent Application 14000855, 2014.
(153) Lyngfelt, A. Solid fuels in chemical-looping combustion—Feeding of fuel and distribution of volatiles. *Proceedings of the 22nd International Conference on Fluidized Bed Conversion*; Turku, Finland, June 14−17, 2015.
(154) Li, X.; Lyngfelt, A.; Mattisson, T. An experimental study of a volatiles distributor for solid fuels chemical-looping combustion process. *Fuel Process. Technol.* **2021**, *220*, 106898.
(155) Leckner, B.; Golriz, M. R.; Zhang, W.; Andersson, B.-Å.; Johnsson, F. Boundary layers—First measurements in the 12 MW CFB research plant at Charmers University. *Proceedings of the 11th International Conference on Fluidized Bed Combustion*; Montreal, Quebec, Canada, April 21−24, 1991; pp 771−776.
(156) Golriz, M. R.; Sundén, B. An Experimental Investigation of Thermal Characteristics in a 12-MW_{th} CFB Boiler. *Exp. Heat Transfer* **1994**, *7* (3), 217−233.

https://doi.org/10.1021/acs.energyfuels.1c03615
Energy Fuels 2022, 36, 9588−9615